



Contrasting seasonal patterns in particle aggregation and DOM transformation in a sub-Arctic fjord

Maria G. Digernes*¹, Yasemin V. Bodur*², Martí Amargant-Arumí², Oliver Müller³, Jeffrey A. Hawkes⁴, Stephen G. Kohler¹, Ulrike Dietrich², Marit Reigstad², Maria Lund Paulsen⁵

5 ¹Department of Chemistry, Norwegian University of Technology, Trondheim, 7049, Norway

²Arctic and Marine Biology, UiT – the Arctic University of Norway, 9019, Norway

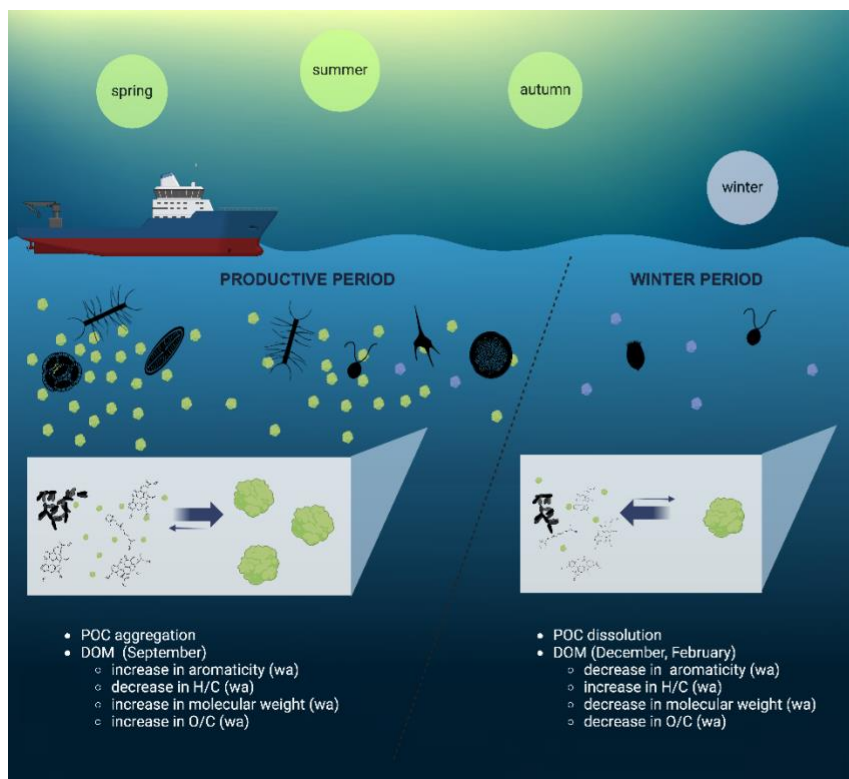
³Department of Biological Sciences, University of Bergen, 78303, Norway

⁴Department of Chemistry, University of Uppsala, 75124, Uppsala

⁵Department of Biology, Aarhus University, 8000, Aarhus

10 *Correspondence to:* maria.g.digernes@ntnu.no, yasemin.bodur@uit.no. *these authors have contributed equally to this work.

Abstract. Particulate (POM) and dissolved (DOM) organic matter in the ocean are important components of the Earth's biogeochemical cycle and in constant dynamic change through physical and biochemical processes. However, they are mostly treated as two distinct entities, separated operationally by a filter. We studied the transition between the DOM and POM pools and its drivers in different seasons in a sub-Arctic fjord by monthly environmental sampling and performing aggregation-
15 dissolution experiments. For the experiments, surface water (5 m) was either pre-filtered through a GF/F filter (0.7 µm), or left unfiltered, followed by 36 h incubations. Before and after the incubation, samples were collected for dissolved and particulate organic carbon concentrations (DOC, POC), microbial community (flow cytometry) and in-depth analysis of the molecular composition of DOM (HPLC-HRMS). During the biologically productive period, when environmental POC concentrations were high (April, June, September), the filtered water showed a rapid increase of POC concentrations by up to 88% within 36
20 h, indicating net-aggregation processes. During this process in September, DOM lability decreased based on changes in average hydrogen saturation and aromaticity of DOM molecules. In contrast, during the winter period (December, February), when environmental POC concentrations were low, the experiments indicated a dissolution of POC with a net-loss up to 58%. Simultaneously, the DOM pool became more labile during the incubation period indicated by changes in average hydrogen saturation, aromaticity, and oxygen saturation. In both periods, bacterial activity increased throughout the incubation, showing
25 that bacterial degradation likely plays a role in the transformation of POM and DOM. Our data highlights the importance of both physically driven DOM aggregation and biologically driven POM dissolution during different periods of the year, together determining the fate of the OM pool in high latitude marine ecosystems.



1 Introduction

30 Dissolved (DOC) and particulate organic carbon (POC) play an important role in earth's biogeochemical cycling, and their availability and variation are strongly driven by seasonal ecosystem dynamics. In the ocean, dissolved organic matter (DOM) makes up 97% of total organic matter, while only 3% is in particulate form (Hansell et al., 2009). Marine DOM is one of the largest stocks of organic carbon on earth, while particulate organic matter (POM) has the potential to sink gravitationally and thus, transport carbon from the ocean surface to the seafloor and hereby contribute to carbon sequestration (Iversen, 2023; Turner, 2015). POM (usually defined as $> 0.4 - 0.7 \mu\text{m}$ until several mm in size) is mostly composed of protist cells, fecal pellets, biogenic leftovers such as mucilaginous feeding nets and DOM that stick together to form large marine snow aggregates. DOM and POM are separated operationally merely by size (nominal filter pore size between 0.2 and $0.7 \mu\text{m}$; Carlson et al., 2015) and often studied independently, despite the constant dynamic change between the two fractions (He et al., 2016; Verdugo et al., 2004; Wells, 1998). DOM does not sink gravitationally; however, it can contribute to the export of biogenic carbon by downward mixing (Hopkinson & Vallino, 2005), aggregation to POM, or formation of a sticky matrix for particles (Engel et al., 2004; Hansell et al., 2009; Iversen, 2023; Wells, 1998). Consequently, DOM provides a particle source which is well known, but often overlooked in ecosystem studies (Engel et al., 2004).

35
40



DOM is primarily generated and secreted by phytoplankton during their growth or through viral lysis, and subsequently utilized
45 as a substrate by microbial organisms (Hansell et al., 2009; Riley, 1963; Wagner et al., 2020). Phytoplankton release 2 – 50%
of the photosynthetically fixed carbon as DOM (Thornton, 2014; Paulsen et al., 2018). DOM is also released during the
degradation of POM. Freshly produced labile DOM exhibits temporal fluctuations in accordance with the seasonal and spatial
variations in phytoplankton abundance, microbial communities, and inorganic nutrient availability (Osterholz et al., 2014;
Paulsen et al., 2019; Retelletti Brogi et al., 2019; Vernet et al., 1998). Labile DOM, which constitutes less than 1% of the
50 overall DOM reservoir, displays relatively short turnover times, typically ranging from hours to days (Hansell, 2013a).
Conversely, seemingly recalcitrant DOM persists in the ocean over more extended time scales, ranging from months to
thousands of years (Fleurs et al., 2012; Hertkorn et al., 2006). Within the recalcitrant DOM category, there is a semi-labile
DOM fraction with turnover times spanning from months to years. Efforts have been made to characterize this semi-labile
DOM pool (Repeta, 2015), however the bulk of DOM characterization studies are mostly conducted in spring and autumn
55 (Flerus et al., 2012; Osterholz et al., 2014; Retelletti Brogi et al., 2019) and thus presenting a need for winter DOM
characterization studies.

Depending on physicochemical and biological conditions, DOM can undergo various transformations, such as aggregation,
dissolution, adsorption, resorption, autoxidation, (photo)chemical and biological degradation (Carlson & Hansell, 2015). These
60 transformations result in alterations of DOM molecular composition, abundance, and size, with implications for the ecosystem
and the carbon cycle. DOM that is channelled through the microbial loop can be transformed to more recalcitrant forms (Jiao
et al., 2010) or converted back to carbon dioxide, while particles that are formed through DOM aggregation can potentially
sink and lead to carbon export. Dissolution of POM to DOM removes OM from the classical food web, decreases the particulate
pool, leads to a longer turn-over time of OM in the water column and decreases the sinking potential. Despite the strong
65 dependency of DOM and POM transformations on ecosystem processes, not much is known about changes in the DOM-POM
continuum under contrasting environmental and seasonal conditions.

Colloids or gels act as the “gray zone” between the dissolved and the particulate fractions (Orellana & Leck, 2015). They can
be characterized as high molecular weight (HMW) DOM (> 1 kDa) but are also often quantified as particulate material as they
70 can remain on filters due to their sticky, flexible properties. More than ¼ of oceanic DOC can be in colloidal form (Kepkay,
1994). Transparent exopolymer particles (TEP) are sticky gels formed from extracellular polymeric substances (EPS) composed
of carbohydrate-rich phytoplankton exudates (Passow et al., 1994; Passow, 2002b). Spontaneous assembly of smaller
molecules can lead to the abiotic formation of gels (Chin et al., 1998; Passow, 2000). These processes can be triggered by
small changes in ambient pH, ionic concentration, temperature, or light (He et al., 2016; Timko et al., 2015; Verdugo et al.,
75 2004). Colloids/gels can aggregate to particulate matter through chemical coagulation or physical flocculation (Engel et al.,
2004). These aggregated particles can form again after filtration of sea water indicated by the presence of POC in dissolved



samples at filtration timescales (Riley, 1963; Sheldon et al., 1967; Valdes Villaverde et al., 2020; Xu & Guo, 2018) and their measurement often appear as an analytical artifact.

80 High latitude ecosystems are characterized by a strong seasonality, creating contrasting environmental conditions (Petersen & Curtis, 1980). Arctic and sub-Arctic fjords can be periodic hotspots for biological productivity, and locations of high carbon production, turnover and export. With the beginning of spring, the return of sunlight and replenished nutrients in the upper water column fuel intense phytoplankton blooms, and with that the production of fresh POM and DOM (Paulsen et al., 2018; Walker et al., 2022; Wetz & Wheeler, 2007). Spring is influenced by autochthonous labile DOM production composed of low oxygen and high hydrogen saturation (Hansell, 2013a). Late spring and early summer are subject to high freshet with allochthonous DOM input from river sources composed of oxygen rich DOM compounds (Koch et al., 2005; Sleighter & Hatcher, 2008). Towards summer, nutrients become depleted at the surface, and the system is dominated by heterotrophic processes and increasing carbon turnover (Carlson et al., 2015; Repeta, 2015). With decreasing nutrient concentrations and increasing abundance of senescent cells, EPS can be excreted at high concentrations and trigger flocculation events during post-bloom conditions in summer (Alldredge & Gotschalk, 1989; Engel, 2000; Hellebust, 1965; Mague et al., 1980; Mari & Burd, 1998; Mykkestad, 1995; Passow, 2002a; Thornton, 2014). In Autumn, DOM is converted to more recalcitrant compounds with lower hydrogen saturation (Osterholz et al., 2014) and there is a decrease in TEP (von Jackowski et al 2020). Autumn mixing in fjords can redistribute nutrients in the water column and fuel autumn blooms later in the year (Vonnahme et al., 2022). During winter, low light conditions limit primary production and the water column is subjected to an increase in vertical mixing. Organic matter concentrations are at their lowest during this period and seemingly recalcitrant due to dissolved organic carbon accumulation (Hansell, 2013b). However, microbial degradation of organic matter can still take place (Vonnahme et al., 2022; Wietz et al., 2021).

100 Studies of the DOM–POM continuum in aquatic environments have mostly been interpreted either from an ecological or a chemical point of view, and most studies were carried out in the laboratory. We are aware of only a few studies that combined laboratory and field observations (Riley, 1963; Sheldon et al., 1967), or associated changes in the DOM–POM continuum with DOM molecular composition and size (Einarsdottir et al., 2020; Xu & Guo, 2018). The overarching aim of this study is to document the effect of DOM–POM processes under contrasting ecological conditions and seasons. This is relevant in a highly seasonal and drastically changing Arctic, to understand possible implications for the carbon cycle and carbon burial. We hypothesize that biologically active periods with higher POM concentrations have a higher potential for aggregation of DOM via adsorption in comparison to the winter period. We further wish to understand a) how the bioavailability of the vast DOM pool was affected by aggregation and dissolution, b) how biological processes impacted the DOM-POM continuum. To test the hypothesis, we closely followed the DOM and POM concentration and character along with a range of environmental parameters during a full annual cycle in the surface water of a sub-Arctic fjord. We designed experiments to examine the partitioning between DOM and POM, by incubating 1) filtered (0.7 μm) fjord water, where biological activity was strongly



reduced and particles removed, and 2) unfiltered water where pre-formed gels, microorganisms and other POM sources were kept as under natural conditions. This allowed us to simultaneously obtain an insight into the net-aggregation processes in the filtered water and the sum of the aggregation + dissolution + biological processes in the unfiltered controls during all seasons. Additionally, we investigated the behavior of extracellular polymeric substances and its link to biological processes and DOM aggregation.

2 Methods

2.1 Sampling of standard and experimental parameters

Fieldwork was conducted on a monthly basis in the mouth of an Arctic fjord close to Tromsø/Romsa (Ramfjorden/Gáranasvuotna; 69°31'34"N, 19°1'33.0"E) between 16.09.2020 and 24.08.2021 with RV Hyas (Fig. 1). Ramfjorden is a sidearm of the larger Balsfjorden, which is mainly influenced by Norwegian Coastal Water, and seasonally by the inflow of Atlantic Water in spring (Eilertsen et al., 1981). Ramfjorden receives allochthonous input mainly through the inflow from two rivers (Storelva and Sørbotnelva). During winter, the inner part of the fjord freezes and is covered by sea ice (O'Sadnick et al., 2020). Sampling for this study occurred in the mouth of the fjord, which was ice-free year-round. In the beginning of each sampling event, a CTD equipped with fluorescence, oxygen and turbidity sensors was deployed. Water samples were taken at 5m depth with a GoFlo (General Oceanics, 20 L). Due to lack of research vessel access in July, we sampled in the beginning and the end of June (08. and 30.06.2021) and hence refer to these sampling events throughout the manuscript as "June" and "July".

From the GoFlo, 15 L were subsampled into a plastic canister for later processing in the lab every month (Fig. 2a-c) for the following biogeochemical parameters: chlorophyll-a (Chl-a), total particulate matter and particulate inorganic matter (TPM/PIM), protist taxonomy, extracellular polymeric substances (EPS) and flow cytometry (FCM). For dissolved organic matter characterization (DOM), water from the same GoFlo was subsampled into a separate acid-washed 3 L canister. Three triplicate samples for dissolved organic carbon (DOC) and total dissolved nitrogen (TDN) were taken with muffled glass vials and for nutrients with 50 mL falcon tubes directly from the GoFlo. All tubing used was acid-cleaned prior to use, and sample containers were pre-rinsed with sample water before sampling.

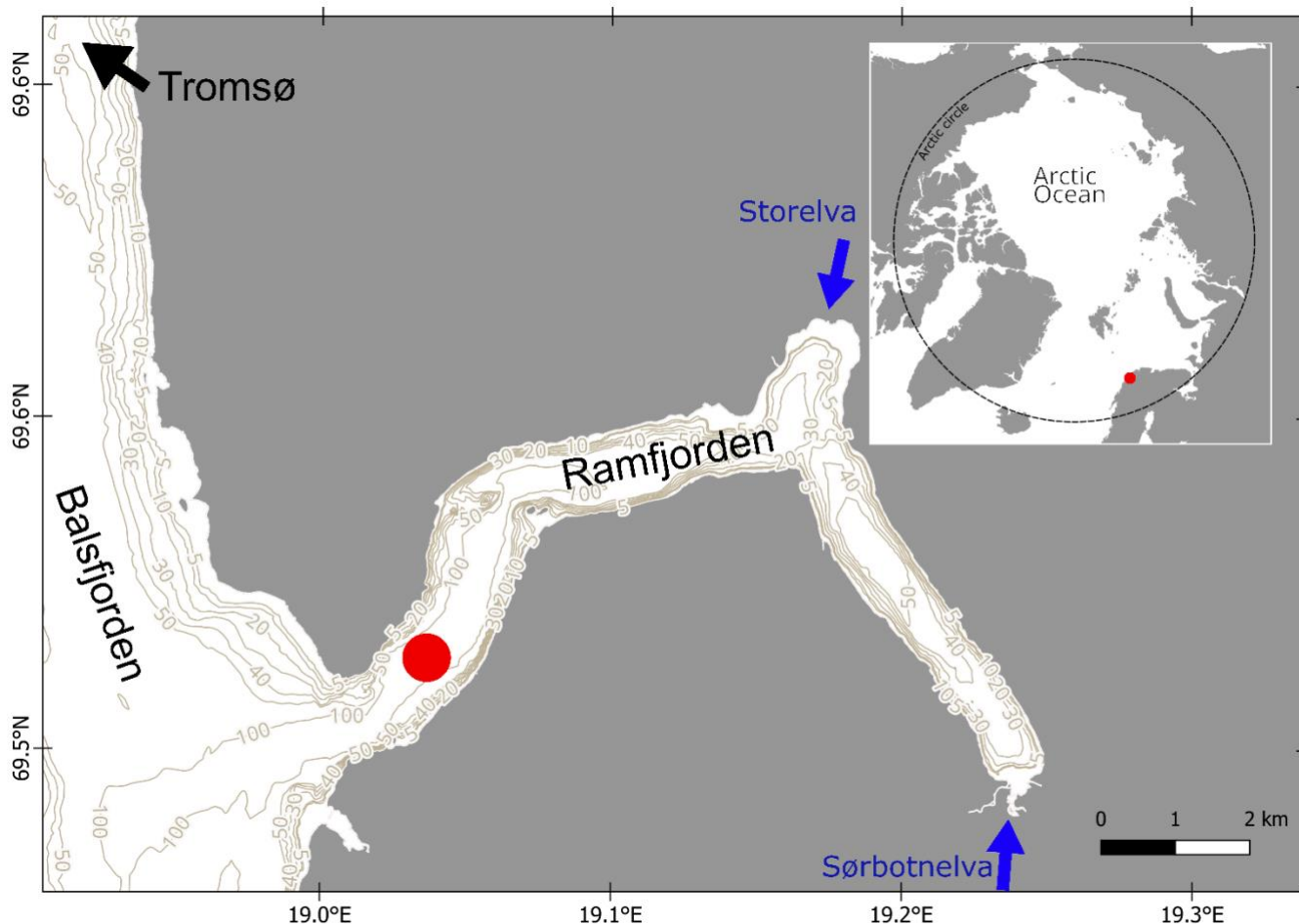


Figure 1: Position of Ramfjorden/Gáranasvuotna within the Arctic Circle and sampling location (red dot) within the fjord. Land area and depth contours of Ramfjorden were retrieved from kartkatalog.geonorge.no.

140 2.2 Aggregation experiment

To demonstrate seasonal contrasts of the aggregation potential of DOM in the fjord, experiments were conducted every second month (Fig. 2d-f). The water from three GoFlos was filtered through a 90 μm mesh to remove large grazers and evenly distributed among 3 acid-washed 20 L canisters after being pre-rinsed with sample water through staggered filling. The canisters were covered with black plastic bags to minimize light exposure. After bringing them on shore, the canisters were stored in a controlled temperature room kept dark at 5°C where the experiments were carried out by using headlamps with red light to reduce the possibility of biological production. Each time prior to the experiments, all surfaces and the floor in the cold room were washed with Citranox® acid detergent and distilled water to remove dust and minimize carbon contamination. Any handling of the samples was carried out wearing microporous laminated clean suits (Tyvek®, DuPont, USA), and all used equipment and tubing was acid-rinsed (plastic equipment), combusted (glass equipment) or cleaned in an ultrasonic cleaner (metal equipment) prior to use.

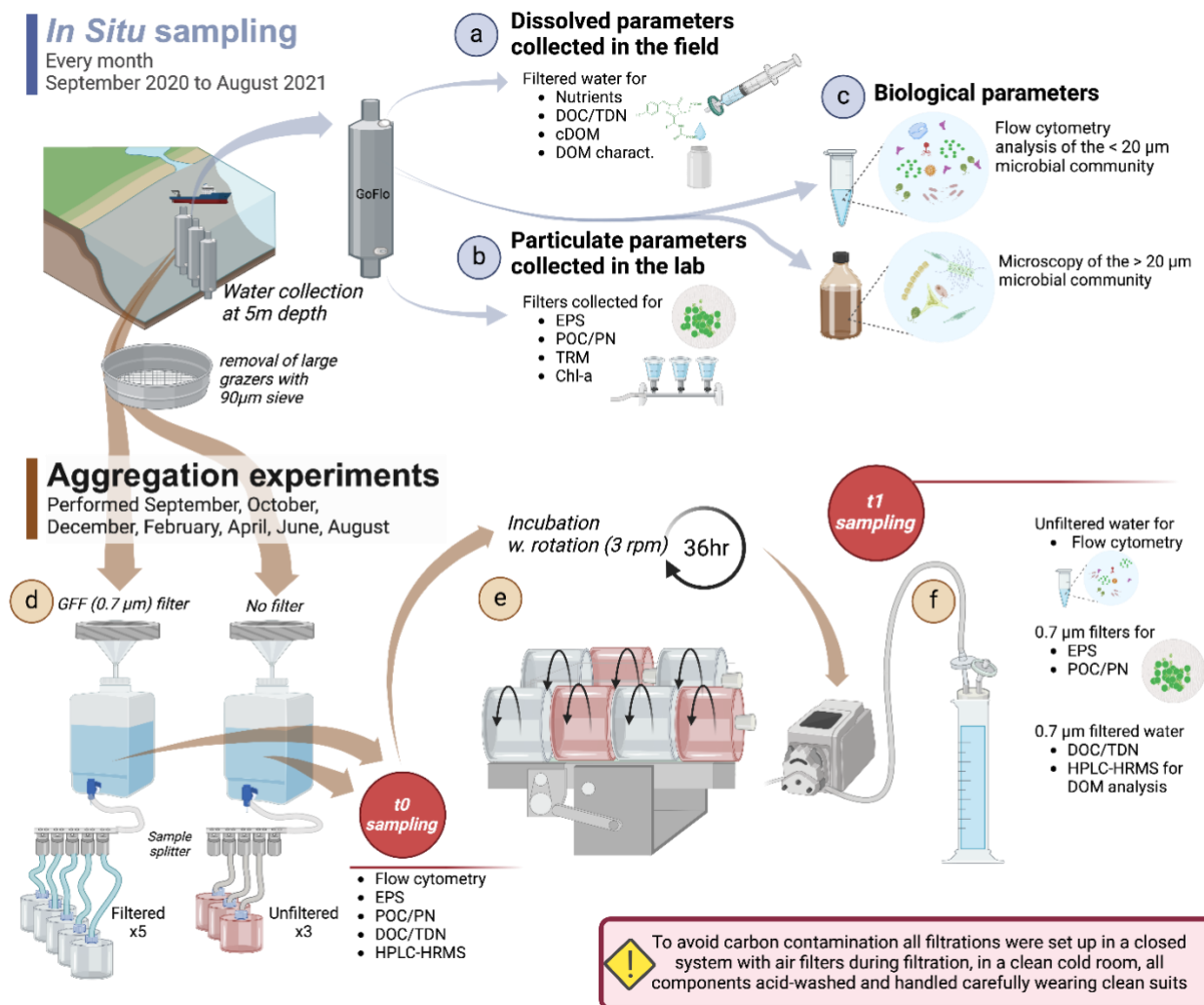


Figure 2: Sampling scheme and experimental setup. Water was sampled with 20L GoFlos at 5 m depth, and the following standard parameters (STD) were collected: (a) nutrients, dissolved organic carbon (DOC), total dissolved nitrogen (TDN), dissolved organic matter characterization (DOM charact.), and colored DOM (cDOM) were taken directly in the field; (b) filters for the analysis of extrapolymeric substances (EPS), particulate organic carbon and particulate nitrogen (POC/PN), total particulate matter (TPM) and Chlorophyll-a (Chl-a) were collected in the lab; and (c) water samples were preserved for protist taxonomy and flow cytometry (FCM). The experimental water was collected from 3 x 20L GoFlos, funnelled through a 90µm sieve and distributed equally among 3 canisters. The experiment was set up as in (d): The experimental water was channelled through a pressure-filtration system with a GF/F filter (filtered; F) and without a GF/F filter (unfiltered; UF), and then sampled respectively for EPS, FCM, DOM, DOC, TDN and POC were taken. Afterwards, the F and UF water respectively were distributed evenly among roller tanks with a sample splitter. (e) During a 36h incubation period, the tanks were rolled at 3rpm. (f) After the termination of the incubation, each tank was subsampled for EPS and FCM. Subsequently, the tanks were connected to a peristaltic filtration system with in-line filters that were used for the sampling of POC. The filtrate was collected in graduated cylinders, which was then subsampled for DOC and DOM characterization.

155

160



165 The water from two canisters was pressure-filtered through a single layer (September, October, December) or a double layer
(February, April, June) of pre-combusted GF/F filters (0.7 μm , Whatman, diameter: 130 mm) which was placed on an acid-
washed plexiglass filter holder and collected in another canister (filtered, F; Fig. 2d). The effect of a double or a single layer
on POC concentrations was tested in January, for the results and a short discussion see the supplementary (Fig. S1). To compare
the aggregation behavior of the filtrate to the behavior of the seasonally changing natural unfiltered water, we left the water
170 from the third canister unfiltered (UF). The water from the third canister was streamlined through the filtration system in the
same way, but without a filter, to account for possible hydraulic stress during the filtration procedure and treat the UF samples
in the same way as F. Filtered treatment (F) samples were collected for POC/PN, EPS, FCM, DOC and DOM characterization
immediately after this step (t_0 samples). UF treatment samples for t_0 were collected for POC/PN, EPS and FCM. It should be
noted that for DOC and DOM characterization, UF treatment at t_0 is equivalent to F treatment at t_0 . Subsequently, the F and
175 UF water was distributed evenly into cylindrical plexiglass tanks (1.8 L self-manufactured, 18 cm inner diameter, 6 cm height)
by using a splitter. The tanks were filled until the top and air bubbles were removed before they were closed with silicone
stoppers. Eight tanks (3x UF, 5x F) were placed on two rolling tables in randomized order and rolled for 36 h at 3 rpm to
ensure a homogenized distribution of the water body throughout the incubation (Fig. 2e).

180 After 36 h, the incubation was stopped, and samples (t_1) were taken from each tank for EPS and FCM after gently
homogenizing the tanks by turning them slowly 20 times. Afterwards, all tanks were connected air-tight (to minimize
contamination) to a peristaltic filtration system where GF/F filters were connected in-line and the filtrate was collected in acid-
washed and equally air-tight graduated cylinders (Fig. 2f). After rinsing the whole system and the graduated cylinders with
sample water, the filters were replaced and the subsequently collected filtrate was used for the subsampling of DOC and DOM.
185 After each tank was emptied completely, the filters were collected for POC/PN analyses in the following way: the tubing of
the lower part of the filter holder was removed, and any excess water in the tubing or in the filter holder was sucked onto the
filter with a syringe. Subsequently, the dry filters were folded, packed into pre-combusted aluminum foil, and frozen at -20°C .
The exact volume used for the subsampling of all the parameters was read from the graduated cylinders. EPS, FCM, DOC,
DOM and POC/PN were analyzed as described in the following section.

190

After the experiment was finalized, all used equipment was soaked in acid for several hours, rinsed three times with MilliQ,
dried in a drying oven at 60°C and finally stored in airtight zip bags or boxes until the next sampling to prevent any carbon
contamination.

2.3 Processing of samples

195 In situ samples for particulate organic carbon (POC) and particulate nitrogen (PN) were filtered in triplicates, and experimental
samples as described in Section 2.2, onto pre-combusted GF/F filters (0.7 μm , Whatman), packed in combusted aluminum foil
and frozen at -20°C . POC samples were dried for 24 h at 60°C , subsequently acid-fumed (HCl) in a desiccator for 24 h to



remove all inorganic carbon, and finally dried again for 24 h at 60°C. The filters were transferred into tin capsules and measured with a CE440 CHN elemental analyzer (Exeter Analytical). Acetanilide was used as standard.

200

Samples for the colorimetric determination of extracellular polymeric substances (EPS) were taken in situ between November 2018-September 2019, and then again between February-August 2021 in situ and for the experiment. We measured EPS instead of TEP directly, because the EPS measurement has a higher detection accuracy for all carbohydrates in a sample (including TEP + TEP precursors) compared to the Alcian Blue method after Passow & Alldredge (1995; Bittar et al., 2018; Li et al., 2018). The sampled water (150ml) was filtered onto 0.4 µm polycarbonate filters. Following the colorimetric method by Dubois et al. (1956), a mixture of phenol and concentrated sulfuric acid was used to extract material from the filter to determine total carbohydrates in the sample. A spectrophotometer (UV-6300PC, VWR) was used to measure the absorbance of the solution at 485 nm. Since concentrations were too low to be calculated reliably with a standard curve against xanthan gum concentrations, relative EPS concentrations are depicted as “absorption at 485 nm”.

210

Flow cytometry was used for the determination of bacteria, virus, pico- and nano-sized phytoplankton abundances in situ and in the experiment. Unfiltered samples of 5 mL were fixed in duplicates with glutaraldehyde (0.5% final concentration) and frozen at -80°C until analysis within 3 months. The samples were thawed and pico- and nanophytoplankton were analyzed directly on an Attune® Acoustic Focusing Flow Cytometer (Applied Biosystems by Life Technologies). The populations of phytoplankton were grouped based on their pigmentation on biplots of green vs. red fluorescence. Before counting bacteria and viruses, the DNA was stained with SYBR-green I and groups were discriminated on biplots of side scatter vs. green fluorescence. Actively dividing bacterial cells contain more DNA, therefore the ratio of High Nucleic Acid (HNA) bacteria to Low Nucleic Acid (LNA) bacteria is here used as an indicator of the relative activity of the bacterial community. The following conversion factors were used to convert various microorganism groups to carbon (pg C cell⁻¹): bacteria (0.02), Synechococcus sp.(0.29), pico eukaryotes (0.57), nanophytoplakton (7).

220

Samples for dissolved organic carbon (DOC) and total dissolved nitrogen (TDN) were filtered on GF/F filters (0.7 µm, Whatman, pre combusted) and acidified to pH 2 (HCl, double distilled, AnalaR® NORMAPUR®, VWR chemicals). Samples were stored at 6°C until analysis. DOC and TDN determination were executed via high temperature catalytic oxidation method using a Total Organic Carbon Analyzer (TOC-L CPH/CPN™, Shimadzu). Potassium hydrogen Phthalate (KHP, Merck) was used for external calibration. Seawater reference samples from the University of Miami (Hansell research laboratory) were analyzed throughout sample runs (repeatability > 95%, n = 78).

225

In situ nutrient samples were syringe-filtered through a 0.2 µm filter upon arrival on shore, the filtrate was collected in a second falcon tube and the samples were immediately frozen at -20°C until further analysis. Concentrations of dissolved silicate, nitrate, nitrite and phosphate were measured with a QuAAtro nutrient analyzer (SEAL Analytical).

230



For the determination of in situ total particulate matter (TPM), particulate inorganic matter (PIM) and particulate organic matter (POM), part of the water from the 15 L canister was filtered in triplicates through pre-combusted and pre-weighted GF/F filters (0.7 μm , Whatman). After filtration, the filters were placed on a pre-combusted aluminum dish and dried for 24h
235 at 60°C in a drying oven. The dry weight was measured on a microscale (Mettler-Toledo MX5) to obtain the weight of TPM, and subsequently combusted in the muffle oven at 450°C for 7 h. Finally, the samples were weighed again to obtain the weight of the remaining inorganic material on the filters. POM was calculated from the difference between the dry weight (TPM) and the combusted weight (PIM) of the material.

240 For the determination of Chl-a and Phaeopigments, water was filtered in triplicates through GF/F filters (0.7 μm , Whatman). In order to quantify the contribution of large (> 10 μm) photosynthetic cells, one sample was filtered through a 10 μm polycarbonate filter. Immediately after filtration, the filters were extracted in 100% methanol at 4°C and in dark between 12 – 24 h. Afterwards, the samples were measured with a pre-calibrated Turner Trilogy fluorometer before and after acidification with 5% HCl after (Parsons et al., 1984). In May, samples were measured with a pre-calibrated Turner AU-10 fluorometer.

245 Chl-a/Phaeopigment ratios were calculated as an indicator for the degradation state of the algal material.

For the in situ determination of protist taxonomy (microphytoplankton and heterotrophic protists), 100 mL was filled into a brown glass bottle and fixed with a mixture of glutaraldehyde-lugol for subsequent identification and counting. Protists were identified to the lowest possible taxonomic level, verified through the World Register of Marine Species (WoRMS) and counted with an inverted light microscope (Nikon Eclipse TE-300 and Ti-S) using the Utermöhl method (Edler & Elbrächter,
250 2010; Utermöhl, 1958).

2.4 DOM sample processing

DOM extraction was performed using solid phase extraction (SPE) following the procedure of (Dittmar et al., 2008) with the addition of pre-soak of SPE sorbent with Methanol (HiPerSOLV CHROMANORM[®], 99.8% VWR chemicals) 4 – 6 h prior to extraction. Fjord water samples were filtered (GF/F Whatman[®], 0.7 μm , pre combusted) and acidified (pH 2 with HCl,
255 double distilled, AnalaR[®] NORMAPUR[®], VWR chemicals). Filtered and acidified samples (1 L) were extracted (at 15 mL/min) with a modified styrene-divinylbenzene polymer sorbent (500 mg PPL, Agilent Bond Elut[™]) and 0.1% v/v formic acid (HiPerSOLV CHROMANORM[®] VWR chemicals) was used for salt removal. Final elution was achieved using methanol (HiPerSOLV CHROMANORM[®], 99.8% VWR chemicals) and stored at –20°C in the dark. SPE-DOC recovery was processed by evaporating methanol extracts and redissolving in ultrapure water (28 – 94% DOC recovery). Procedural blanks
260 were processed using ultrapure water (HiPerSOLV CHROMANORM[®], VWR chemicals) and followed the same procedure as samples.



2.4.1 Mass spectrometry analysis

DOM samples were analyzed by high performance liquid chromatography coupled to high resolution mass spectrometry (HPLC-HRMS). Liquid chromatography was performed using an Agilent 1100 Series system with a polar C18 column (Kinetex®, 2.1 x 150 mm, 2.6 µm bead size, 100 Å pore size) with mobile phase (A) 0.1% formic acid in LCMS grade water and (B) 0.1% formic acid in 80:20 acetonitrile : LCMS grade water (v/v). Samples were diluted in 5% v/v Acetonitrile solution (LiChrosolv, Merck) and 20 µL was injected at an initial flow rate of 150 µL min⁻¹ with mobile phase (A) at 95% and mobile phase (B) at 5%. After 10 minutes, the Acetonitrile mobile phase (B) was increased to 95% for 2 minutes and then decreased to 5% where it was held isocratic until 15 min. Mass spectrometric analysis was completed via an LTQ-Velos-Pro Orbitrap MS (Thermo Scientific, Germany) using an electrospray ionization source (ESI) operating in negative mode (spray voltage: -3.1kV, capillary temperature: 275 °C). Blanks consisting of mobile phase A were injected periodically between samples. Each spectrum was internally calibrated in lock mass mode using three expected compounds capsaicin, fusidic acid sodium, glycyrrhizic acid ammonium salt with 304.1921, 515.3378, and 821.3965 negative m/z respectively, providing suitable accuracy and precision (< 1 ppm) in the mass range 150 – 800 m/z. Data was collected at a resolution mode of 100000. More detailed instrumentation parameters are reported elsewhere (Fonvielle et al., 2023).

2.4.2 DOM data processing

Mass spectrometry data were exported from the mass spectrometer and converted to mzXML files with ReAdW then processed further using MATLAB (version 2019b). A MATLAB routine was developed in-house and available with raw mzXML files. Molecular formulas were assigned between 150 – 800 Da masses. Formulas were limited with the following criteria: Carbon (4 – 50), Hydrogen (4 – 100), Oxygen (2 – 40), Nitrogen (0 – 2), Sulfur (0 – 1), H/C = 0.3 – 2.2, O/C = 0 – 1, DBE-O = -10 – 10, valence electron must be equal to an even number, and formulas which contained both nitrogen and sulfur, ¹³C and nitrogen or sulfur and ¹³C were removed. A mass error of 0.7 ppm was allowed for formula assignment. Peak intensities with formula assignments were normalized to sum 1 x 10⁶ for each sample. Further descriptions for the different DOM parameters are given in Table 1.

Table 1: Explanation of DOM parameters used in this study.

DOM Proxy	Description	Explanation	References
O/C ratio	Oxygen to carbon atomic ratio	Older DOM is generally higher in oxygen content due to bacterial and photo-oxidation processes. Higher O/C values can thus indicate a decrease of DOM bioavailability. Terrestrial DOM also contains more oxygen relative to marine DOM.	(Flerus et al., 2012)



H/C ratio	Hydrogen to carbon atomic ratio	A measure for the relative hydrogen saturation. More aliphatic molecules (higher H/C) are more energy rich thus indicate higher DOM bioavailability.	(Cai & Jiao, 2023) and references therein
DBE	Double-bond equivalent. Double-bond containing formulas. Sum of unsaturation plus rings in a molecule	Double-bonds are more difficult to break up (more energy is needed for breaking down the compound); therefore, higher DBE values typically indicate a decrease in DOM bioavailability.	(Cai & Jiao, 2023) and references therein
AI _{mod}	Modified Aromaticity index. Describes poly-aromatic hydrocarbons.	More aromatic rings in DOM molecules lead to a higher AI and indicate low bioavailability and high recalcitrance. DOM of high AI are mostly found in deep waters.	(Koch & Dittmar, 2006a)
MW	Molecular weight	A measure for the size of DOM molecules which give insight into reactivity.	(Flerus et al., 2012)
CHO/S/N	Carbon, hydrogen, oxygen /sulfur/ nitrogen containing formulas	Heteroatoms in organic formulas such as nitrogen and sulfur contain nutrient rich components necessary for microorganisms	

2.5 Statistical analyses

In order to visualize the seasonal biogeochemical cycle in Ramfjorden, a PCA was performed on standardized biological (POC, POC/PN, protist abundance and biomass, FCM data, Chl-a) and environmental (temperature, salinity) variables which were available for all months (except November) between September 2020 and August 2021. Subsequently, a similarity profile routine (SIMPROF) analysis (Clarke et al., 2008) was applied to the same dataset to identify significant clusters of the sampling months (significance level $\alpha = 0.5$) based on the biogeochemical parameters. This allowed us to divide the seasonal cycle in Ramfjorden into distinct biogeochemical periods without prior grouping of the samples.

295

Since DOC samples from the start of the incubations (t₀) were missing for April, we performed a t-test to check whether the DOC collected for the standard parameters and the DOC collected from t₀ of the experiment were significantly different from each other. The two datasets did not show significant differences between each other ($p = 0.54$). Consequently, we used the standard DOC values as t₀ for the experiment during April.

300

All statistical analyses were performed with the computing environment R (Version 4.2.2 (R Core Team, 2018) and the Software Past 4 (Version 4.14, 2022 (Hammer, 2001))).



3. Results

3.1 The seasonal biogeochemical cycle in Ramfjorden

305 In winter, fluorescence was low throughout the whole water column (0.7 - 1 RFU) and density, turbidity and oxygen saturation did not show changes with depth (Fig. S3). PIM values were slightly higher in the winter months (around 0.5 $\mu\text{g}/\text{mL}$ between October - February, except for December) compared to the rest of the year (0.12 - 0.32 $\mu\text{g}/\text{mL}$; Fig. S2a1). Nutrients were increasing from November on and peaked in March, from 2.75 in November to 6 μM in March (Nitrate), 0.2 - 0.5 μM (phosphate) and 2.1 - 4.6 μM (silicate; Fig. S2g-i). By contrast, nitrite peaked in October with 0.1 μM , decreased until January
310 (0.05 μM), and increased again until April (0.08 μM). Chla:Phaeopigments were lowest in December and January and started to increase already in March (Fig. S2w). In April, DOC, Fluorescence, turbidity, TPM, POC, Chla, protist abundance, bacterial abundance and activity as well as nano- and picophytoplankton abundances increased sharply, along with a strong drawdown of nutrients (nitrate: 0.4 μM , phosphate: 0.1 μM , silicate: 1.5 μM ; Fig. S2). Nitrite followed this trend later in May (0.03 μM ; Fig. S2f). Hereafter, nutrient concentrations remained low (Nitrate < 1 μM , Phosphate < 0.3 μM) throughout the summer. In
315 April, over 80% of the total Chla was > 10 μm . Chla and POC decreased in May (0.9 mg m^{-3} and 10 μM , respectively), coinciding with a sharp peak in virus abundance, but increased again in June (6.62 mg m^{-3} and 35 μM , respectively) when also bacterial abundance and activity were highest. DOC and Chla:Phaeo followed this trend. DOC peaked in August (233 μM). Another, lower peak of Chla and POC was observed in September (4.4 mg m^{-3} and 18 μM , respectively). POC made up less than 17% of total OC during the whole year, with highest percentages in June, July and September. POC:PN ratios were highest
320 in March (> 10) and lowest in April (~5; Fig. S2z). Between May and October, POC:PN ratios remained comparable.

Most of the year, the microphytoplankton community was dominated by the diatom genus *Chaetoceros* (Fig. S2x). In April, communities were dominated by both *Chaetoceros* sp. and the prymnesiophyte *Phaeocystis pouchetii* (up to 4×10^5 cells mL^{-1}), in June by *Chaetoceros filiformis*, *Thalassiosira* and *Pseudo-nitzschia* and in July mainly by *Pseudo-nitzschia*. Unidentified
325 flagellates and *Chaetoceros lacinosus* dominated in August, while September was dominated by ciliates (especially *Strombidium conicum*) and various dinoflagellates, that can be mixotroph. The contribution of picophytoplankton was relatively low, with the highest abundance of *Synechococcus* sp. was observed in autumn (max 15000 cells mL^{-1} , Fig. S2r), while the highest abundance of picoeukaryotes was observed in April (9000 cells mL^{-1}).

330 The PCA based on the described environmental and biological variables shows a clear seasonal pattern in Ramfjorden (Fig. 3). Along PC1, which explained 51.28% of the total variance, a clear distinction between winter - autumn - spring was present. During winter, there were elevated levels of nutrients and POC/PN ratios, with the highest concentrations of silicate and phosphate occurring prior to the bloom in March. In April, POC levels, bacterial activity (HNA/LNA) and protist abundance reached their peak with the onset of the spring bloom. The second peak in June was characterized by highest bacterial
335 abundance and high Chla/Phaeopigment ratios. Along the second PC axis (explaining 17.3 % of the variance), spring and



winter are separated from summer and autumn (August, September, October). Here, the biological production becomes increasingly regenerated and is characterized by highest virus abundances and bacteria of low HNA/LNA and dead phytoplankton. During this time, the water temperatures are highest (Fig. S3) and nitrite concentrations exhibit a peak (Fig. S2f). Moreover, salinity is lowest, most likely due to increased runoff from land and precipitation (Fig. S3).

340

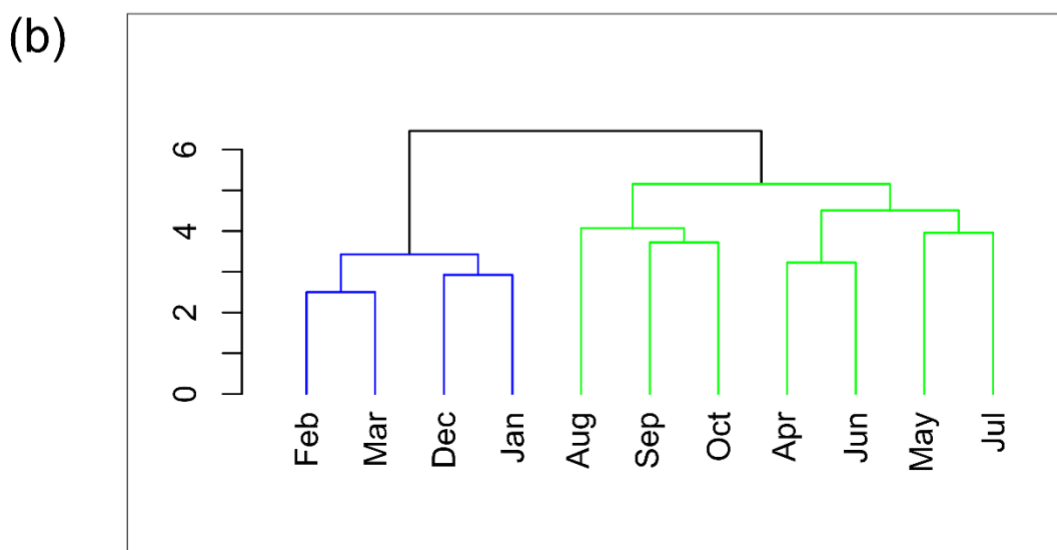
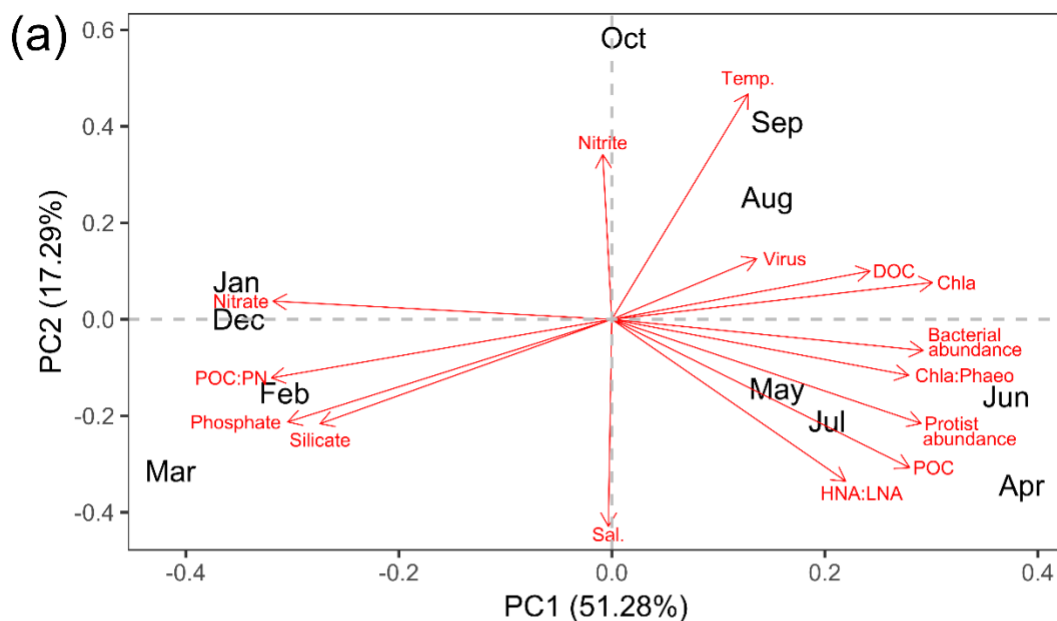




Figure 3: The environmental and biological characterization of Ramfjorden (Tromsø, Norway) between September 2020 and August 2021. a) Visualization of the Principal component analysis (PCA) performed on environmental and biological data (in red) collected every month between September 2020 and August 2021 in Ramfjorden. b) Visualization of the similarity profile routine analysis (SIMPROF) based on the same environmental parameters (euclidian-distance based, significance threshold $\alpha = 0.05$).

345

The SIMPROF analysis in Fig. 3b based on environmental and biological data delineates two seasonal phases of the Ramfjorden ecosystem: a period of high biological activity between April - October (hereafter referred to as “productive period”), and a period with limited light availability for phytoplankton production between November - March (hereafter referred to as “winter period”). Within the “productive period”, a spring scenario (April, June, July) is separated from a summer/autumn scenario (August, September, October; however, this separation is not significant in the SIMPROF analysis). In the following, we are describing the processes in the DOM–POM continuum as observed in our experiment during the two contrasting scenarios (“productive period” and “winter period”) in the fjord environment.

350

3.2 Experimental results

3.2.1 Aggregation-dissolution of particulate organic carbon (POC) and related parameters

355

The change of POC concentrations from the start (t_0) to the end of the incubation (t_1) of filtered (F) and unfiltered (UF) treatments followed a general similar pattern (relative increase or decrease) throughout the year (Fig. 4). After 36 h of incubation, POC concentrations in F water decreased by a mean of $-2.55 \mu\text{M} \pm 0.8$ (around -50% relative to t_0) in winter (December and February). There was an increase of POC during the incubation period in the filtered water (F) of April, June, and September with a mean of $+1.6 \mu\text{M} \pm 0.5$ (Fig. 4; April: 76% increase relative to t_0 ; June: 88%; September: 70%). The decrease in POC in winter and the relative increase in April was followed in a similar manner in UF water (t_0 is not available for UF in September). However, in June, the relative increase of POC concentrations was 4 times higher in UF compared to F.

360

Bacterial biomass in F water did not show large differences after the incubation relative to the start (t_0) from September until April, however they increased in June and August (Fig. 4b). The patterns were different in UF water, where in winter, a decrease of bacterial biomass was observed, while in spring and summer, there was an increase (Fig. S4). Despite performing the incubation in darkness there was an increase in pico-sized phytoplankton cells in the unfiltered (UF) fraction in August. At this time the system had highest concentration of small phytoplankton ($< 2 \mu\text{m}$); picoeukaryotes and *Synechococcus* the summer months and they increased from 2,000 to 15,000 cells mL^{-1} and 4,000 to 26,000 cells mL^{-1} e.g. from 4,000 cells at T_0 to 24,000 cells mL^{-1} after 36hr (Fig. S4), equalling a biomass increase of ca. $2 \mu\text{M}$ carbon (Fig. 4c).

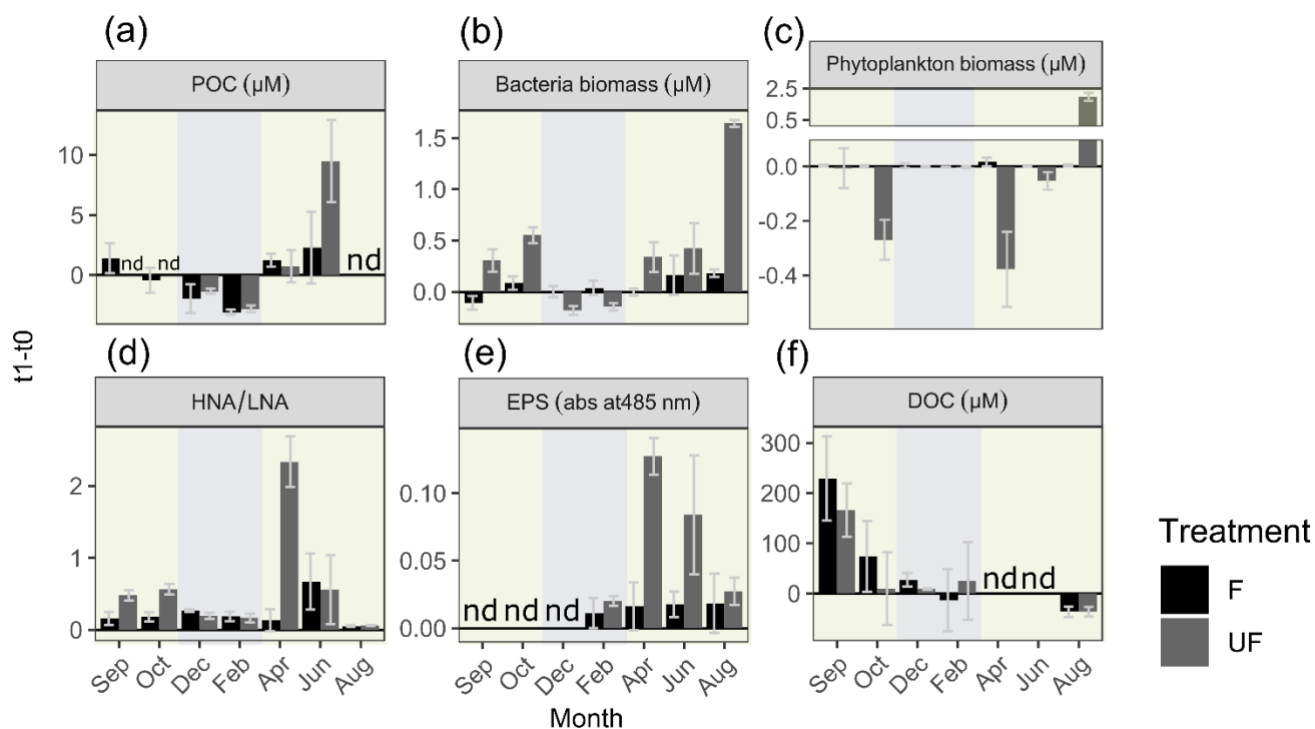
370

In F water, bacterial activity (HNA/LNA) increased relatively constant throughout the year, while in UF water, little change was observed in winter and August, while April was characterized by a sharp increase in activity (Fig. 4d). Similar to bacterial activity, EPS always increased in both treatments and throughout the whole year (sampling apart from February; Fig. 4e).



375 Conspicuously, while for UF water the highest increase in POC was observed in June, the highest increase in EPS was observed in April. In F water, the highest increase in EPS was present in June.

Initial (t_0) DOC concentrations followed a similar pattern as the concentrations in the field (Fig. S2, S4). In September, concentrations increased in both, F and UF water (about +200 μM ; Fig. 4f). In October and December, DOC concentrations still increased in F water (+73.6 to +27.2 μM , respectively), but increased very little or even decreased in UF water. In April and June, DOC concentrations decreased in F, but increased in UF water (Fig. 4f). Molecular composition results of F and UF treatments in the incubation experiments showed similar molecular patterns as seen in Fig. 6 and Fig. S1 and will be discussed further in Section 3.2.2.



385

Figure 4: Change of experimental parameters over the course of the incubation. Change of concentrations from start relative to end of incubations (and their standard deviations; $n = 2-5$) of (a) particulate organic carbon (POC), (b) bacteria biomass (μM), (c) phytoplankton biomass (μM), (d) change of ratio of high nucleic to low nucleic acid bacteria (HNA/LNA) (e) change of concentrations of extracellular polymeric substances (EPS; in relative absorption at 485 nm) and (f) dissolved organic carbon (DOC) (μM). F = filtered water, UF = unfiltered water, nd = no data. The background colors indicate the statistically identified winter (blue) and biologically productive (green) period, respectively.

390



3.2.2 DOM patterns in autumn and winter in relation to aggregation

The molecular composition of DOM was analyzed at the beginning and end of incubation experiments conducted during contrasting periods of the year. September incubations represent a productive period, whereas experiments in December and February indicate a winter period. Additionally, October incubations were also analyzed for DOM composition to assess the transitional period. Variables for DOM composition were reported as signal intensity weighted average (wa) values; thus seemingly small changes in weighted average values point to greater changes in thousands of DOM formulas per sample. Weighted average standard deviations are high compared to average differences between treatments due to the many compounds with different ratios per sample. The high number of detected compounds, however, gives certainty that the weighted average is high (i.e. the standard error of the mean is low), thus making small differences between samples significant (Table 2).

Table 2: High resolution mass spectrometry results of DOM variables showing mean intensity weighted average of hydrogen to carbon (H/C_{wa}), oxygen to carbon (O/C_{wa}), molecular weight (MW_{wa}) and modified aromaticity index ($AI_{mod\ wa}$). SD= standard deviation of weighted mean. N = 3 for the start of incubation (t0) and N = 1 for the end of incubation (t1) (36 hours) for filtered (F) water treatment.

Treatment	$H/C_{wa}(SD)$	$O/C_{wa}(SD)$	$MW_{wa} (SD)$	$AI_{mod\ wa}(SD)$
Sep t0	1.31 (0.24)	0.49 (0.14)	361.40 (74)	0.21 (0.12)
Sep t1	1.25 (0.21)	0.52 (0.12)	365.09 (68)	0.24 (0.12)
Oct t0	1.27 (0.21)	0.51 (0.13)	364.53 (71)	0.23 (0.12)
Oct t1	1.27 (0.22)	0.51 (0.14)	361.95 (70)	0.22 (0.12)
Dec t0	1.28 (0.20)	0.51 (0.13)	369.83 (71)	0.22 (0.11)
Dec t1	1.29 (0.20)	0.51 (0.13)	366.95 (68)	0.22 (0.11)
Feb t0	1.28 (0.20)	0.51 (0.14)	366.05 (69)	0.22 (0.11)
Feb t1	1.30 (0.22)	0.50 (0.13)	363.38 (68)	0.21 (0.11)

During the productive period, studied in the September incubations, average hydrogen to carbon atomic ratios (H/C_{wa}) decreased for both UF and F treatments (Fig. 5). Simultaneously, the average aromaticity ($AI_{mod\ wa}$) and oxygen to carbon atomic ratios (O/C_{wa}) increased for both F and UF treatments (Fig. 5). Average molecular weight (MW_{wa}) increased at the end of incubation in F treatment and decreased at the end of incubation for UF treatment. Notably, a removal of more saturated compounds ($H/C > 1.5$) is observed at the end of incubation (t1) for F (Fig. 6a) and UF (Fig. S5) treatments.

Molecular weight patterns are shown in mass spectra (Fig. 7b) where a decrease in relative intensities of low molecular weight compounds is observed from start (t0) to end (t1) of September incubations for F treatment. These low molecular weight compounds ($< 250\ m/z$) are highlighted on Fig. S6 and show formulas with higher relative intensities at H/C_{wa} ratios greater than 1.3.

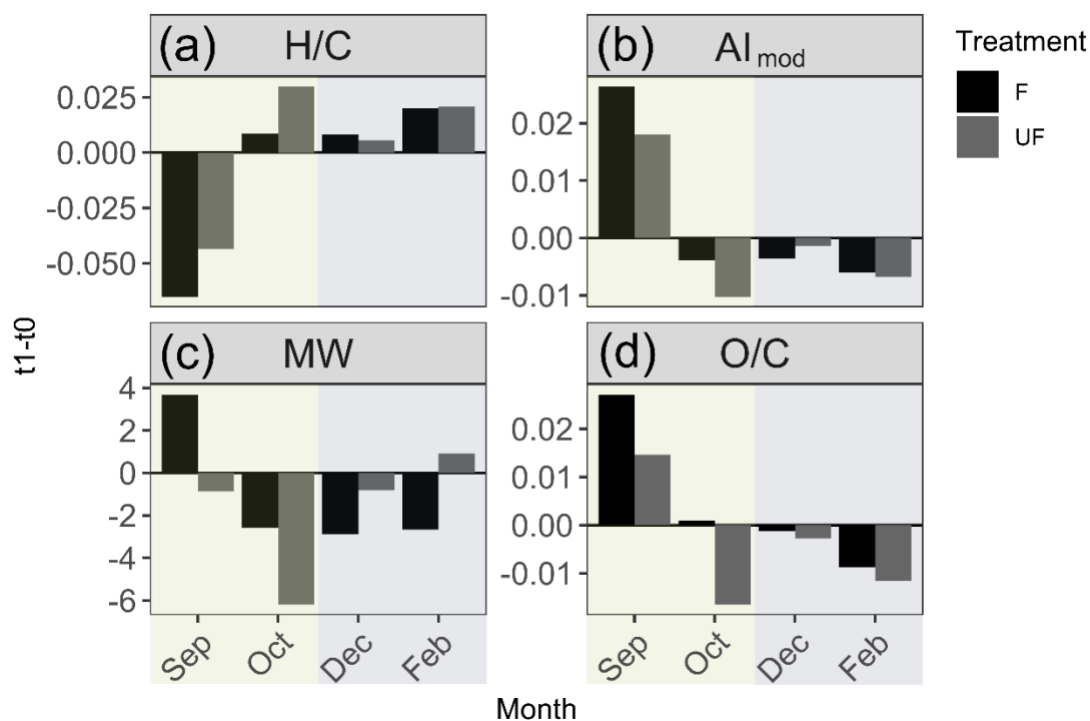


Winter months (December, February) incubations showed a contrasting pattern with an increase in hydrogen saturated
 420 formulas (H/C_{wa}) in both F and UF treatments (Fig. 5 c) d)). During the same period, a decrease in average aromaticity (AI_{mod}
 wa) and oxygen rich formulas (O/C_{wa}) was observed in both F and UF treatments (Fig. 5). Molecular weight (MW_{wa}) decreased
 during the incubation period in the F treatment and increased during UF incubation (Fig. 5). Moreover, there was a decrease
 of less saturated formulas ($H/C < 1.6$) in both F treatment (Fig. 6) and UF treatment (Fig. S5) and slight increase in intensities
 of more saturated formulas for F (Fig. 6) and UF treatment (Fig. S5) at the end of incubation ($t1$).

425

Additionally, changes in DOM variables for October incubation show transitional patterns from spring to winter months (Fig.
 5) with the decrease in formulas that consist of a wide range of H/C ratios (Fig. 6b).

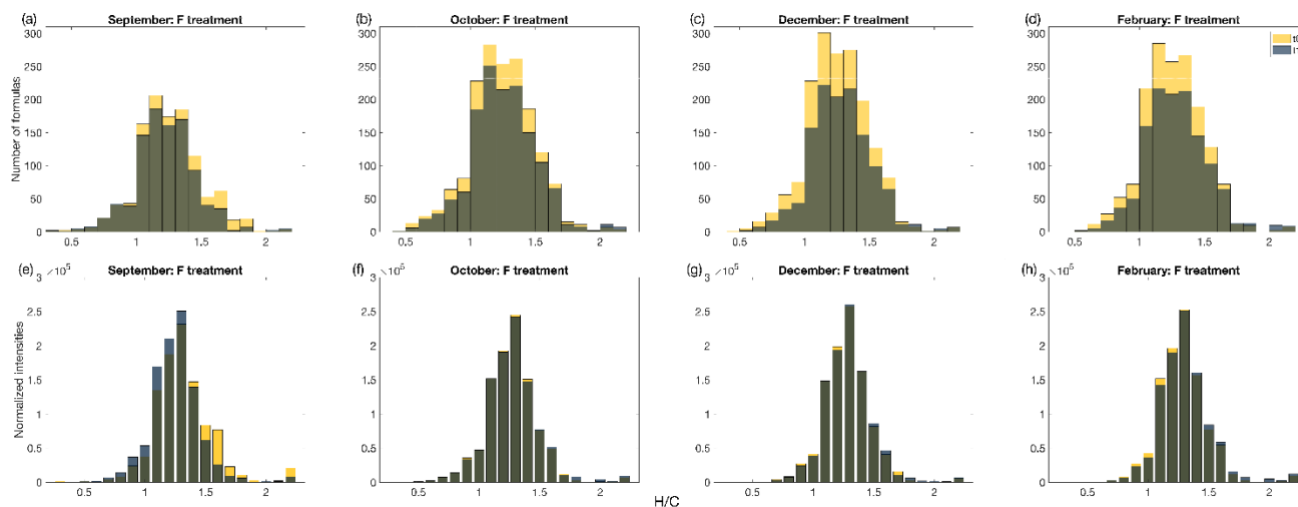
Molecular weight patterns are shown in mass spectra for winter incubations (Fig. 7c) where a decrease in relative intensities
 430 of higher molecular weight compounds is observed at the end of incubation ($t1$). The molecular ratios of formulas higher than
 570 m/z are shown in Fig. S6 composed of formulas in the mid O/C and H/C region of the van Krevelen diagram.



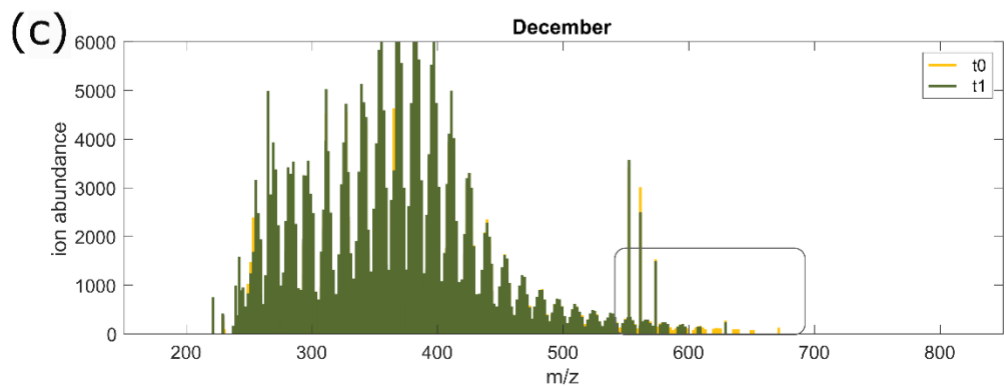
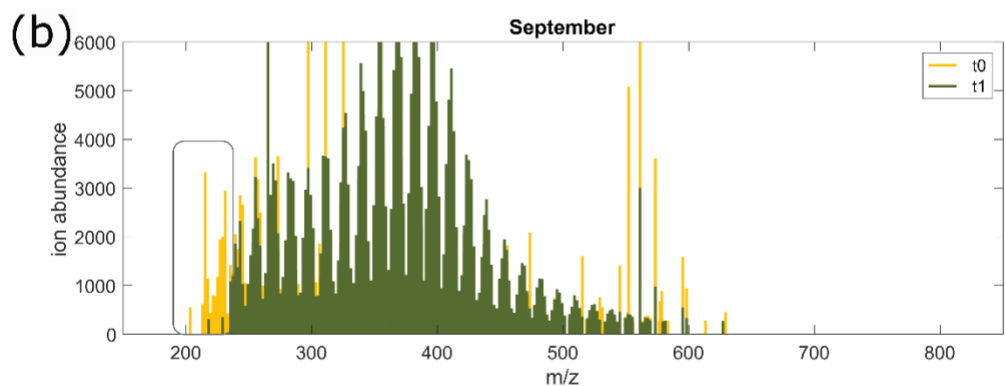
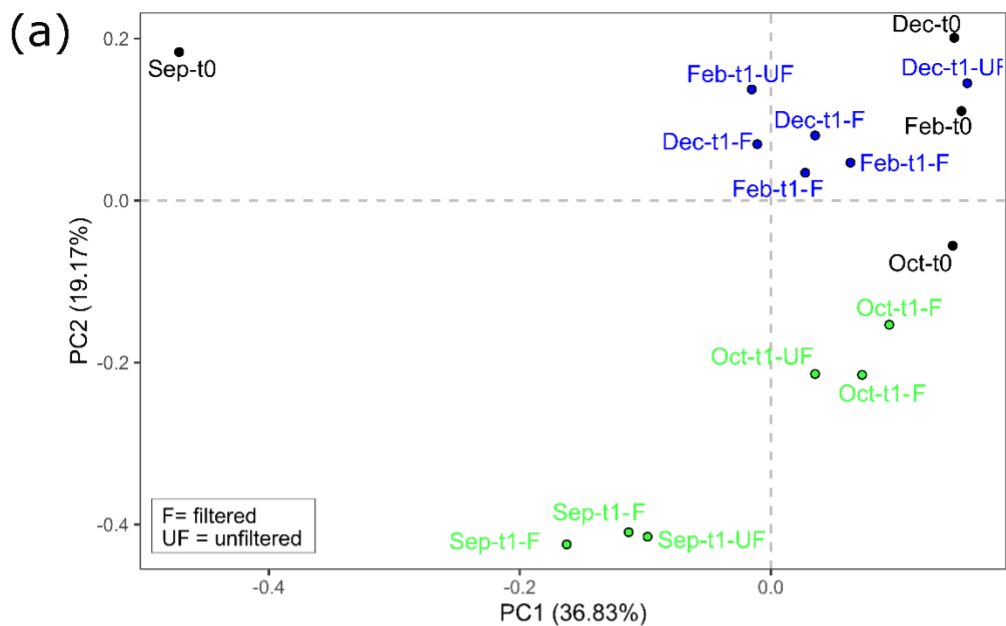
435 **Figure 5: Change of DOM parameters during experiment incubations.** a) change in intensity weighted average DOM parameters in seawater at $t1$ relative to $t0$. a) molecular weight (MW), b) oxygen to carbon ratio (O/C), c) hydrogen to carbon ratio (H/C), d) modified aromaticity index (AI_{mod}). The first treatment is filtered (F) seawater at start and end of incubation ($t1 - t0$) and the second treatment is



unfiltered (UF) seawater for the duration of the incubation then filtered immediately prior to sampling and compared to filtered at the start (t0) incubation (t1 – t0).



440 **Figure 6: Identified organic matter formulas and normalized intensities determined by high-resolution mass spectrometry during**
start (t0) and end (t0) of incubations of F treatment water. Histograms of all identified molecular formulas are plotted according to the
hydrogen to carbon (H/C) atomic ratio for incubation experiments in a) September, b) October c) December and d) February. Normalized
intensities of identified formulas are shown according to the hydrogen to carbon (H/C) atomic ratio for incubation experiments in e)
September, f) October, g) December and h) February. The start of the incubation (t0) is shown in yellow and overlaid with the end of the
445 incubation (t1) in blue (appears green when overlapping with t0). F treatment refers to filtered water (0.7 μm) at the start and end of incubation
(36 h). September shows a decrease in formulas and intensities with higher H/C ratios (> 1.5) whereas winter months (December, February)
show decrease of formulas with low and middle range H/C ratios during incubation period. October indicates a transition period with loss
of formulas across H/C ratios. Changes in intensities and formulas for UF treatment can be found in Fig.S5.





450 **Figure 7: Mass spectra results from the aggregation experiment for F treatment.** a) Visualization of PCA performed on DOM mass spectra from all samples from the experiment. Mass spectra of filtered treatment samples from b) September at t0 (yellow) and overlay t1 (green); and c) December t0 (yellow) and overlay t1 (blue). Changes between incubation periods are highlighted in the rectangles with decrease in molecular weight ($m/z < 250$ Da) in September from the start of incubation (t0) relative to end of incubation (t1) and decrease in high molecular weight in ($m/z > 600$ Da) in December from start (t0) relative to end of incubation (t1).

455 5 Discussion

5.1 The seasonal biogeochemical cycle in Ramfjorden

The spring bloom in Ramfjorden and other close fjords is initiated at the end of March/ beginning of April within a deeply mixed water column (Riebesell et al., 1995; Vonnahme et al., 2022; Walker et al., 2022); this study). The sharp increase of DOC, fluorescence, turbidity, TPM, POC, Chl-a, protist abundance, bacterial abundance and activity (HNA/LNA) as well as nano- and picophytoplankton abundances in April, along with a strong drawdown of nutrients demonstrates the onset of the spring bloom. Consequently, the water becomes turbid due to the increase of organic particles (Fig. S3, Fig. S2) and the photosynthetic activity elevates oxygen concentrations, which is consumed in the following months due to increasing heterotrophic activity (Fig. S3). Hereafter, nutrient concentrations remained low (Nitrate < 1 μ M, Phosphate < 0.3 μ M) throughout the summer. In September, an autumn bloom can develop (Vonnahme et al., 2022) and high zooplankton biomass can occur (Coguiec et al., 2021). Presumably, an autumn bloom developed in September during our study as well, because POC concentrations, standing stocks of total Chl-a, contributions of large cells (Chl-a > 10 μ m) and protist abundance were similar to concentrations in April and July (Fig. S2u, v, x, y).

During winter (December – March), photosynthetic activity was inhibited due to the polar night, and accordingly particulate organic matter, protist abundance and biomass as well as Chl-a concentrations were at their minimum (Fig. S2u, x). The water column is deeply mixed between December and April (Fig. S3), displaying no changes in density, turbidity and oxygen saturation with depth, and nutrients were redistributed, as demonstrated by elevated nutrient concentrations in the surface water. Despite low biological activity, bacteria continue to decompose the available algal remains during this period (Vonnahme et al., 2022). This is also supported by the high POC/PN and low Chl-a/Phaeopigment ratios of organic particles during winter, which demonstrate that they were in a regenerated state (Fig. S2w, z).

5.2 Aggregation in the biologically active period

The increase of POC concentrations in filtered (F) water during the “productive period” (April-September) suggests that aggregation of the dissolved fraction is promoted when primary production occurs, and phytoplankton exudates increase DOM concentrations in the aquatic environment. This has been described in other studies (Alldredge & Jackson, 1995; Burd & Jackson, 2009; Engel et al., 2004; He et al., 2016 and references therein; Orellana & Leck, 2015 and references therein; Passow, 2002b and references therein). During winter (December and February), on the other hand, POC concentrations in both F and unfiltered (UF) water decreased, suggesting a “dissolution” of particles. Our study represents the first seasonal investigation



of the DOM-POM continuum. It is important to note, however, that we found the increase in POC did not lead to a simultaneous decrease in DOC (Fig. 4c), the reasons for which will be discussed further below in Section 5.3.2.

485 5.2.1 Mechanisms of the transformation of DOM into POM

Previous studies have shown that large (up to 5 μm) polymer gels and particulate material can be reformed quickly after they have been removed from filtered sea and river water, despite consecutive filtrations and at different filter sizes (0.2 μm , 0.4 μm or 0.7 μm ; Chin et al., 1998; He et al., 2016; Kerner et al., 2003; Passow, 2000, 2002b; Sheldon et al., 1967; Valdes Villaverde et al., 2020). Even when bacteria are killed, microgels of sizes between 200 nm to 1 μm can form within 30 min, and up to 5 μm after 50 h (Chin et al., 1998; Kerner et al., 2003; Sheldon et al., 1967). The same process cannot be observed in filtered artificial seawater, but addition of dissolved carbon enhances aggregation (Gruber et al., 2006; Sheldon et al., 1967). Several studies and reviews have pointed out the ability of DOM to assemble spontaneously into polymer gels, which can aggregate to particles (Chin et al., 1998; Engel & Passow, 2001; Passow, 2000; Valdes Villaverde et al., 2020). We suggest that the same process occurs during the present study, when we observe an increase of POC after 36 h in filtered (F) water taken during the biologically productive period between April and September. For the first time we show the seasonality of this aggregation process.

DOM concentrations are elevated through phytoplankton production, which is why we observe aggregation during the biologically productive period. In situ EPS concentrations, representative for large sugars (> 0.4 μm) follow the same seasonal pattern as protist abundance (Fig. S2t,x). Diatoms dominated the phytoplankton community during the peak Chl-a periods in April and June (Fig. S2x). In April, the mucous colony forming prymnesiophyte *Phaeocystis* sp. also comprised a major fraction of the phytoplankton community of Ramfjorden, and during this period EPS was elevated (0.84 relative absorption at 485 nm; Fig S2t). It was also in April that we saw the largest increase in EPS during the 36h incubation, indicating that the residues from *Phaeocystis* sp. are especially prone to reform into EPS. In contrast, in June when only diatoms dominated (Pseudo-nitzschia sp. and *Chaetoceros* filiformis) the experimental production of EPS was approximately 30% lower, despite peak in situ concentrations of EPS in June (1.91 relative absorption at 485 nm, Fig. S2t).

Table 3. Percentage of particulate organic carbon (POC) contribution from aggregation of filtered (F) and unfiltered (UF) treatments relative to the in situ POC concentrations. ΔF and ΔUF refer to the end of incubation subtracted by the start of the incubation value for each respective treatment (F and UF).

Month	In situ POC (μM)	ΔF POC (μM)	ΔUF POC (μM)	% F POC of in situ POC	% UF POC of in situ POC
September	17.82	1.40	n.d.	7.88	n.d.
October	13.62	-0.44	n.d.	-3.23	n.d.



December	3.95	-1.98	-1.36	-50.12	-34.56
February	4.02	-3.11	-2.83	-77.22	-70.48
April	74.43	-1.24	0.73	1.67	0.98
June	79.96	2.28	9.49	2.86	11.87

Aggregation from the dissolved pool (increased POC in F water) accounted for between 1.7% (April) and 7.9% (September) of the POC concentrations measured in the field (Table 3). Other studies showed that up to 35% of particulate matter present in situ can be formed in filtered water through aggregation (Riley, 1963; Sheldon et al., 1967); however, this occurred over longer time scales (several days vs 36 h in our experiment) and by the addition of shear. Phase shifts from DOM to POM are
515 mainly driven by physical processes such as Brownian motion, chemical changes (e.g. ambient pH, ionic concentrations, temperature, light, bridging with divalent cations) and/or physical stress such as turbulent shear (e.g. filtration), differential settling, surface coagulation (e.g. bubbling) or bacterial motility (Engel & Passow, 2001; He et al., 2016; Kepkay, 1994; Passow, 2000; Timko et al., 2015; Valdes Villaverde et al., 2020; Verdugo et al., 2004). During our experiment, shear was probably only introduced during the filtration and at the beginning and the end of the rotation. During the incubation, the
520 rotation merely ensured the equal distribution of the material within the tank. Still, within a short amount of time (36 h), we measured increased POC concentrations in F water during the biologically productive period of the year.

DOM–POM processes are usually driven by bacterial degradation (dissolution of POM), and physical processes (aggregation to POM or defragmentation). Our seasonal study shows that although bacterial activity increased during the incubation period
525 in all months, microbial processes during the productive period seem to play a lesser role in the DOM–POM transition compared to physical aggregation. Other studies have similarly shown that while POC concentrations remain constant after consecutive refiltrations, bacterial abundances decrease, bacterial activity remains low and substrates that are preferred to bacterial degradation can accumulate (Engel et al., 2004; Valdes Villaverde et al., 2020). Addition of sodium azide to inhibit microbial activity does not change the coagulation behavior of polymers, but the addition of EDTA, which disperses microgels
530 and polymers, inhibits coagulation (Chin et al., 1998). These examples support that aggregation mainly stems from physical rather than biological transformation. Similarly, Engel & Passow (2001), Passow (2000), and Valdes Villaverde et al. (2020) show that gels > 0.4 μm in size form efficiently under shear and hydraulic stress. Overall, during the biologically productive period, a substantial fraction of particulate material can originate from the DOM pool, and changes in the DOM–POM continuum (in the direction of aggregation) have shown to be dominated by aggregation processes uncoupled from bacterial
535 activity.

Changes in DOM composition during the incubation period for F and UF treatments were similar compared to the start of incubation (t_0) and indicated little effect of larger organic size fractions (0.7 – 90 μm) on the composition of DOM during the 36h incubations (Fig. 6 & Fig. S5). However, DOM compositional changes at t_1 relative to t_0 were contrasting for productive



540 versus winter period regardless of treatment, thus indicating that DOM compositional changes were driven by abiotic process and/or microbial communities in the dissolved fraction ($< 0.7 \mu\text{m}$). Due to similarities between F and UF treatments (Fig. 6 & Fig S5), we primarily focus on discussing F treatment in DOM composition sections unless otherwise stated.

5.2.2 Decreased DOM lability and increased molecular weight during September

Molecular composition analysis of DOM in September of F treatment indicates the removal of more saturated formulas and decrease in intensities of these formulas ($\text{H/C} > 1.4$; Fig. 6a) during the incubation time of the experiment and could be explained by microbial degradation and/or abiotic aggregation of saturated compounds. Simultaneously, an increase in average aromaticity ($\text{AI}_{\text{mod wa}}$) of DOM compounds was observed during incubation and is likely due to the removal of saturated molecules which tend to be low in aromaticity (Koch & Dittmar, 2006a). These changes indicate a decrease in the average lability of DOM compounds during September incubations (D'Andrilli et al., 2015, 2023). Notably, the removal of low molecular weight compounds ($< 250 \text{ Da}$) was also observed in mass spectra at start of incubation (t_0) versus end of incubation (t_1 ; Fig. 7). These low molecular weight compounds at the start of incubation are mainly composed of higher H/C saturation ($\text{H/C} > 1.3$; Fig. S6); thus, removal of these compounds could explain lower average H/C_{wa} ratios observed. Microbial degradation of these compounds ($< 250 \text{ Da}$) is contrary to the size reactivity continuum which proposes higher reactivity of DOM as molecular weight increases (Benner & Amon, 2015). Particularly, aggregation of highly saturated DOM has been observed for larger fractions, such as polysaccharides (Passow, 2000; Passow et al., 1994), which are outside of our mass spectrometry analysis window, yet can indicate aggregation patterns of saturated functional groups. Also observed an increase in microbial activity along with an increase in molecular weight compounds. Thus, abiotic aggregation of low molecular weight compounds, supported by the increasing experimental POC concentrations during our incubations, could be an explanation for the decrease in average saturated compounds, despite the large molecular size difference between these two fractions. Xu & Guo (2018) showed that $\text{DOC} < 1 \text{ kDa}$ was mainly responsible for the formation of particles ($> 0.45 \mu\text{M}$).

Average oxygenation of molecules (O/C_{wa}) also increased during the incubations in September. This could be due to the removal of low O/C (< 0.5) and high H/C ratio (> 1.5) formulas as seen in Fig. S8 instead of the production of highly oxygenated compounds. Although Maie et al. (2008) have shown aggregation of highly oxygenated compounds, our experimental results did not show this.

5.2.3 Enhanced aggregation under post-bloom conditions

POC aggregation during the experiment was higher in June compared to April (increase by $1.2 \mu\text{M}$ POC in April vs. $2.6 \mu\text{M}$ in June for F, and an increase of $0.7 \mu\text{M}$ in April vs. $9.5 \mu\text{M}$ in June for UF water). Higher aggregation under post-bloom conditions in June compared to April were not surprising, as EPS accumulate under increasing nutrient limitation and/or with increasing concentrations of senescent cells, as it is the case during post-bloom conditions in summer (Engel, 2000; Hellebust, 1965; Mague et al., 1980; Mykkestad, 1995; Passow, 2002b; Riebesell et al., 1995; Thornton, 2002). EPS are released already



in the growth phase of phytoplankton during the initiation of a bloom; however, most EPS are probably present in the form of LMW compounds in the beginning of a spring bloom (Paulsen et al., 2018). This is supported by higher field DOC concentrations in April than in June, while field concentrations of EPS, which are representative for large polysaccharides (> 575 0.4 μm), were lower in April compared to June (Fig. S2t). This might also explain why in April both treatments, F and UF, had a similar increase of POC levels relative to start of incubation (increase of 1.24 and 0.73 μM ; respectively), although initial POC concentrations at the start of incubation (t_0) were 11 times higher in UF than in F water. Despite particle concentrations being high, little precursor material was probably present in UF water to promote aggregation in the beginning of a bloom compared to a post-bloom scenario.

580

Later, in June, we observed a 9 times higher aggregation potential of UF water compared to April, while we only observed a 1 times higher aggregation potential of F water (Fig. 4a). In summer, towards the end of a bloom, not only does the field concentration of EPS increase, but also the concentration of suspended particles as shown by an increase of POC and TPM in the field (Fig. S2y,a1). Because coagulation becomes more likely when a critical concentration of particles is reached, 585 aggregation is usually enhanced under post-bloom conditions (Burd & Jackson, 2009; Dam & Drapeau, 1995; Mague et al., 1980; Passow, 2002b; Thornton, 2014). Colloids can be scavenged by larger particles (Druffel et al., 1992; Kepkay, 1994) and can even lead to enhanced carbon sedimentation (Forest et al., 2013; Riebesell et al., 1995). Higher POC and EPS concentrations in the field during June likely increased the chance of organic matter to coagulate in UF water. Interestingly, however, experimental POC concentrations in UF water were higher in April compared to June. This might indicate that the 590 concentration of precursor material plays a more critical role for aggregation than particle concentration. Our experiment suggests a higher contribution of DOM to the POM pool during summer compared to spring, and a higher aggregation potential in general (as seen in UF water) during a post-bloom compared to a peak-bloom scenario. It should be noted, however, that experimental EPS concentrations at the start of incubation (t_0) in UF water were consistently an order of magnitude lower than the respective field EPS concentrations, which indicates that a large fraction of EPS was retained on the 90 μm sieve and 595 therefore not included in the experiment, probably because of their sticky nature. Therefore, we likely did not adequately replicate aggregation in truly unfiltered water, and our measurements can be considered as conservative estimates for aggregation in unfiltered water.

5.3 Particle dissolution in winter

Our experiment shows a decrease in POC concentrations in F and UF water after incubation during winter (December and 600 February). In the ocean, particles are usually remineralized in the pelagic zone due to solubilization by bacteria, sloppy feeding by zooplankton or fragmentation (Iversen, 2023; Kiørboe, 2001; Svensen & Vernet, 2016). Photo-dissolution can also turn POM into dissolved material, especially in surface waters under direct light influence (Pisani et al., 2011). Since large grazers were filtered out and the experiments were carried out in the dark, we propose that bacterial degradation was responsible for the observed dissolution patterns of organic matter that was present in the winter water. This is also supported by the increase



605 of bacterial activity in the experiment at t_1 relative to the start of incubations (t_0) throughout the year, and by the fact that we observed dissolution in F and UF water.

Other aggregation experiments conducted in temperate regions where light is still available during winter show that particles form from filtered water during this time of the year (Riley, 1963; Sheldon et al., 1967). Our study, however, measured a decrease in POC concentrations during winter and changes in DOM composition (see Section 5.3.1) at the end of incubation
610 compared to the start of incubation (t_0) which could indicate that this dissolution process occurs in the Arctic polar night, but not in temperate regions. However, we also measured an increase in experimental EPS concentrations in the F water during February. This might indicate that several processes take place in the DOM-POM continuum during winter as well. Our results indicate that dissolved EPS molecules ($< 0.45 \mu\text{m}$) are aggregating, while at the same time POM is degraded by bacteria. For
615 instance, (Xu & Guo, 2018) showed that DOM compounds in a certain size range aggregated simultaneously while other DOM compounds were degraded by bacteria.

Experimental POC concentrations at the start of incubation ($4.7 - 5.3 \mu\text{M}$ in F, and $5.6 - 6.0$ in UF water; Fig. S4) were similar to field POC concentrations in winter (around $4 \mu\text{M}$, Fig. S2y), which suggests that particles were of extremely low abundance
620 and size during the winter period. Throughout the whole sampling period (September-August), experimental POC concentrations at t_0 in UF water largely followed a similar seasonal pattern as field POC concentrations, although at lower levels. However, experimental POC concentrations at t_0 in F water seemingly followed opposite patterns, with low concentrations in September ($2 \mu\text{M}$) increasing in winter until February ($5.3 \mu\text{M}$) and sharply declining in April ($1.6 \mu\text{M}$). A possible explanation is that during filtration of water with high particle and EPS abundance, as is the case in the productive
625 period, small molecules are retained on the filter because they get trapped in the sticky matrix or aggregates, therefore don't pass the filter pores and lead to lower POC concentrations in F water at t_0 during the productive period compared to higher POC concentrations at t_0 the winter period.

5.3.1 Increased DOM lability and decreased molecular weight during winter incubations

DOM molecular composition analysis during winter incubations (December and February) indicate a decrease in unsaturated
630 DOM (Fig. 6) and an increase in relative intensities of more saturated DOM (H/C; Fig. S8). Moreover, average aromaticity ($AI_{\text{mod wa}}$) decreased during this period, which could be due to the removal of low H/C DOM which is typically of higher aromaticity (Koch & Dittmar, 2006b). These observations indicate an increase in average lability of DOM and could be due to the dissolution of POC observed during this period as it can lead to the production of more labile DOM. Additionally, there was a significant decrease of a group of low H/C compounds referred to as 'terrestrial peaks' (t-Peaks) (-15 t-Peak formulas,
635 $p = 0.008$, $n = 9$). T-Peaks are a group of compounds that are commonly present in vastly different rivers as reported by Medeiros et al., (2016; Fig. S7). Removal of these compounds could contribute to the increase in average H/C_{wa} ratios observed in winter incubations. This suggests a potential degradation of t-Peak compounds during winter, in contrast to September when



t-Peaks did not significantly change during the incubation. Arctic winter microbial communities differ substantially from spring, summer and autumn communities (Marquardt et al., 2016; Vonnaehme et al., 2022; Wietz et al., 2021), and therefore
640 the winter community is likely better adapted to degrade various carbon sources, while summer communities are specialized in degrading phytoplankton derived DOM as shown in Wilson et al (2017). These findings support that terrestrial DOM is an important carbon source for bacteria during winter in Ramfjorden (Vonnaehme et al., 2022), which has implications for the fate of riverine DOM in sub-Arctic fjords and a freshening Arctic Ocean.

645 Additionally, there was a removal of relatively higher molecular weight compounds (570 – 700 Da) as shown in mass spectra (Fig. 7c). These higher molecular weight compounds were in the mid O/C and H/C ratio region of the van Krevelen diagram (Fig. S6) which are typically rich in carboxyl groups (Broek et al., 2020; Hertkorn et al., 2006). We suggest that the decrease of these compounds could indicate colloid formation of higher molecular weight (> 700 Da) as it has been previously observed for carboxyl rich organic matter (Chin et al., 1998). However, experimental POC concentrations during the incubations indicate
650 a dissolution, and not an aggregation of particles during the winter. This could be due to the low relative intensity of these higher molecular weight compounds (570 – 700 Da), thus no detection of increased POC concentrations during this period.

5.3.2 An unbalanced carbon budget

Throughout the experiment, we expected that DOC and POC would behave antagonistically, and thus an increase in POC would see a corresponding decrease in DOC, resulting in a stable amount of total organic carbon (TOC; sum of DOC and
655 POC), as observed in other aggregation studies (Engel et al., 2004). However, this was not always the case during our experiments; the most pronounced unbalance of the carbon budget was an increase in both DOC (+229 μ M) and POC (+1 μ M) in September. This suggests that our experiment was either not a closed system, or that there was an interchange with the inorganic C pool. Notably, experimental DOC values of ultra-pure water blanks show average DOC concentrations of 53 μ M \pm 30 (mean \pm SD) and DOM molecular analysis of ultrapure water experimental blanks reveal relatively low number of
660 contamination peaks (average number of peaks: 123 \pm 33, mean \pm SD), thus not affecting DOM characterization results and ruling out contamination as a source of significant carbon addition. Moreover, the DOC concentrations measured in the experiment are well within the range of the in situ measurements (ranging from 87-233 μ M; Fig. S2k).

In winter months the carbon budget had a slight net-loss of TOC (POC + DOC) as observed in February, which was most
665 likely due to bacterial respiration of OM to CO₂. In both October and December, a decrease in POC (-0.4 μ M and -2 μ M, respectively) did reflect an increase in DOC (+74 μ M and +27 μ M, respectively), however indicating a substantial additional source of DOC. The high increase in TOC observed mainly in September, but also in October and December could be partly explained by carbon fixation in the dark by phytoplankton, as Vonnaehme et al. (2022) describe extremely low, but measurable primary production during winter in Ramfjorden. While this may play a role in the unfiltered treatments where phytoplankton
670 was abundant, it is unlikely to explain an increase in the filtered treatment (abundances of picophytoplankton < 200 cell mL⁻¹



675 ¹). In the filtered treatments we did however observe a rapid increase in the activity of bacteria, presumably as in this fraction they were released of grazing pressure from bacterivorous protists. Further, viruses are present in the filtered treatment and at their peak abundance (up to 1.3×10^7) in autumn. Viruses have a significant role in controlling microbial population (Suttle, 2007), which during the lytic stage can lead to a substantial production of DOM through viral lysis of microorganisms (Chen et al., 2022). We hypothesize that the significant production of DOC observed in September in the filtered treatment may be due to viral lysis of the otherwise rapidly growing bacterial community (relieved from grazing pressure, and not limited by carbon nor nutrients). In the unfiltered treatment the presence of phytoplankton (new production) may explain the increase in DOC, while the presence of protist grazers results in a less efficient lysis of bacterial cells, and therefore a net lower production of DOC (Moran 2022). However, this does not solely explain the overall increase in organic carbon in our autumn and winter 680 experiments, and further investigations should be made to resolve the underlying mechanisms, and we here flag that viral lysis in the autumn may lead to unexpectedly high DOC production.

6 Conclusions and Outlook

685 With increasing water temperatures and increasing terrestrial runoff, a greater portion of DOM is expected to be released into the Arctic Ocean (Nguyen et al., 2022; Thornton, 2014). This can have consequences for the dynamic physical, biological and chemical processes occurring in the DOM-POM continuum. With its sharp seasonal gradients, the Arctic presents a suitable place to study the influence of different environmental factors on DOM–POM dynamics. Our experiment demonstrates that transitions in the DOM–POM continuum are subject to seasonality at high latitudes and behave very differently in the productive period compared to winter.

690 In winter (December and February), we observed an increase in average DOM lability potentially through the solubilization of particles, as indicated by the dissolution of POC. OM availability in the Arctic is limited during low production periods in the polar night and our results indicate that during this time under low particle concentrations, dissolution of particles is the dominant process. This contrasts with other observations that show aggregation during winter in a temperate region (Riley, 1963), and is possibly because temperate systems are not light-limited and primary production (and with that, EPS exudation) 695 can take place throughout the year, even if it is reduced. However, these findings may extend beyond the Arctic's polar night, suggesting that similar processes in the DOM-POM continuum might be occurring in regions with periods of low production such as oligotrophic ecosystems. Studying the seasonality of DOM-POM processes is therefore crucial to understand carbon cycling in the ocean.

700 Additionally, there was a decrease in DOM compounds in the 570 - 700 Da molecular weight range at the end of incubation (t_1) during winter, which could indicate colloidal formation of carboxyl-rich compounds. A significant decrease in so-called terrestrial peaks in winter has implications for removal of river DOM. However, more work is needed to disclose the



mechanisms involved. Arctic microbial communities in winter are different from spring and summer communities (Marquardt et al., 2016; Vonnahme et al., 2022; Wietz et al., 2021) and could be responsible for the different processes observed during
705 winter. We propose that the dissolution of POC and degradation of unsaturated DOM are occurring in winter to produce more labile DOM during a period with low DOM production.

During the “productive period” (April-September) we observed POC aggregation which correlated with the removal of highly saturated DOM of low molecular weight in September. This suggests the formation of aggregates from saturated DOM of low
710 molecular weight. At the same time, bacterial activity increased during the incubations, as average DOM was transformed to more recalcitrant DOM. October incubations showed a transitional period between productive and winter months with a decrease in labile DOM and increase in recalcitrant compounds. These findings underline that a substantial fraction of POM can originate from the DOM pool through aggregation, although bacterial degradation is taking place simultaneously. Aggregation within short time frames in the productive period (within 36 h as we have shown, and probably shorter)
715 demonstrate that standard POC measurements in the field under periods of high production likely underestimate actual in situ POC concentrations, as they do not account for the dynamic exchange with the DOM pool.

Author contributions

MGD and YVB equally lead the study design, field work, data analysis and writing of the article. MLP and MAA contributed to the study design and sample analysis. MAA took part in field work and was responsible for the sampling and analysis of
720 the field parameters. MGD was responsible for the dissolved, and YVB for the particulate and biological parameters of the experiment. MLP analysed FCM and cDOM samples. JAH contributed to the sample and data analysis of DOM, and UD analysed EPS samples. SGK contributed to field work and sample analysis. The draft of the manuscript was written by YVB, MGD and MLP, and all authors contributed to the interpretation of the data and commented on the manuscript. All authors read and approved the final manuscript.

725 Competing interests

The authors declare no conflict of interest.

Acknowledgements

We would like to thank the crew of R/V Hyas who made it possible to collect samples every month. We thank Reidar Kaasa and Per Gjerp for manufacturing the experimental equipment and Evald Nordli for logistics. We thank Camilla Svensen, Lena
730 Seuthe, Rolf Gradinger and Tobias Vonnahme for their input regarding the experimental setup and fieldwork, and Tobias



Kielland, Lena Seuthe, Elisabeth Halvorsen and Anna Miettinen for help in the field and in the lab. We also would like to thank Anna Maria Dąbrowska for the taxonomic identification of protists. This study was funded by the Research Council of Norway (#276730) through the Nansen Legacy project (MGD, YVB, MAA, SGK, OM, MR). The work was also funded by the Norwegian university of science and technology (NTNU; MGD, SGK) and The Arctic University of Norway (UiT; YB, MAA).

References

- Allredge, A. L. and Gotschalk, C. C.: Direct observations of the mass flocculation of diatom blooms: characteristics, settling velocities and formation of diatom aggregates, *Deep Sea Research Part A. Oceanographic Research Papers*, 36, 159–171, [https://doi.org/10.1016/0198-0149\(89\)90131-3](https://doi.org/10.1016/0198-0149(89)90131-3), 1989.
- 740 Allredge, A. L. and Jackson, G.: Aggregation in marine systems, *Deep Sea Research (Part II, Topical Studies in Oceanography)*, 42, 1–7, 1995.
- Benner, R. and Amon, R. M.: The size-reactivity continuum of major bioelements in the ocean, *Ann Rev Mar Sci*, 7, 185–205, <https://doi.org/10.1146/annurev-marine-010213-135126>, 2015.
- 745 Bittar, T. B., Passow, U., Hamaraty, L., Bidle, K. D., and Harvey, E. L.: An updated method for the calibration of transparent exopolymer particle measurements: Updated TEP calibration method, *Limnol Oceanogr Methods*, 16, 621–628, <https://doi.org/10.1002/lom3.10268>, 2018.
- Broek, T. A. B., Walker, B. D., Guilderson, T. P., Vaughn, J. S., Mason, H. E., and McCarthy, M. D.: Low Molecular Weight Dissolved Organic Carbon: Aging, Compositional Changes, and Selective Utilization During Global Ocean Circulation, *Global Biogeochemical Cycles*, 34, e2020GB006547, <https://doi.org/10.1029/2020GB006547>, 2020.
- 750 Burd, A. B. and Jackson, G. A.: Particle Aggregation, *Annual Review of Marine Science*, 1, 65–90, <https://doi.org/10.1146/annurev.marine.010908.163904>, 2009.
- Cai, R. and Jiao, N.: Recalcitrant dissolved organic matter and its major production and removal processes in the ocean, *Deep Sea Research Part I: Oceanographic Research Papers*, 191, 103922, <https://doi.org/10.1016/j.dsr.2022.103922>, 2023.
- 755 Carlson, C. A. and Hansell, D. A.: Chapter 3 - DOM Sources, Sinks, Reactivity, and Budgets, in: *Biogeochemistry of Marine Dissolved Organic Matter (Second Edition)*, edited by: Hansell, D. A. and Carlson, C. A., Academic Press, Boston, 65–126, <https://doi.org/10.1016/B978-0-12-405940-5.00003-0>, 2015.
- Carlson, C. A., Hansell, D. A., Hansell, D. A., and Carlson, C. A.: DOM Sources, Sinks, Reactivity, and Budgets, in: *Biogeochemistry of Marine Dissolved Organic Matter*, Elsevier, 65–126, <https://doi.org/10.1016/B978-0-12-405940-5.00003-0>, 2015.
- 760 Chen, X., Wei, W., Xiao, X., Wallace, D., Hu, C., Zhang, L., Batt, J., Liu, J., Gonsior, M., Zhang, Y., LaRoche, J., Hill, P., Xu, D., Wang, J., Jiao, N., and Zhang, R.: Heterogeneous viral contribution to dissolved organic matter processing in a long-term macrocosm experiment, *Environment International*, 158, 106950, <https://doi.org/10.1016/j.envint.2021.106950>, 2022.
- Chin, W.-C., Orellana, M. V., and Verdugo, P.: Spontaneous assembly of marine dissolved organic matter into polymer gels, *Nature*, 391, 568–572, <https://doi.org/10.1038/35345>, 1998.
- 765 Clarke, K. R., Somerfield, P. J., and Gorley, R. N.: Testing of null hypotheses in exploratory community analyses: similarity profiles and biota-environment linkage, *Journal of Experimental Marine Biology and Ecology*, 366, 56–69, <https://doi.org/10.1016/j.jembe.2008.07.009>, 2008.
- Coguiac, E., Ershova, E. A., Daase, M., Vonnahme, T. R., Wangensteen, O. S., Gradinger, R., Præbel, K., and Berge, J.: Seasonal Variability in the Zooplankton Community Structure in a Sub-Arctic Fjord as Revealed by Morphological and Molecular Approaches, *Frontiers in Marine Science*, 8, 2021.
- 770 Dam, H. G. and Drapeau, D. T.: Coagulation efficiency, organic-matter glues and the dynamics of particles during a phytoplankton bloom in a mesocosm study, *Deep Sea Research Part II: Topical Studies in Oceanography*, 42, 111–123, [https://doi.org/10.1016/0967-0645\(95\)00007-D](https://doi.org/10.1016/0967-0645(95)00007-D), 1995.



- 775 D'Andrilli, J., Cooper, W. T., Foreman, C. M., and Marshall, A. G.: An ultrahigh-resolution mass spectrometry index to estimate natural organic matter lability, *Rapid Communications in Mass Spectrometry*, 29, 2385–2401, <https://doi.org/10.1002/rcm.7400>, 2015.
- D'Andrilli, J., Romero, C. M., Zito, P., Podgorski, D. C., Payn, R. A., Sebestyen, S. D., Zimmerman, A. R., and Rosario-Ortiz, F. L.: Advancing chemical lability assessments of organic matter using a synthesis of FT-ICR MS data across
780 diverse environments and experiments, *Organic Geochemistry*, 184, 104667, <https://doi.org/10.1016/j.orggeochem.2023.104667>, 2023.
- Dittmar, T., Koch, B., Hertkorn, N., and Kattner, G.: A simple and efficient method for the solid-phase extraction of dissolved organic matter (SPE-DOM) from seawater, *Limnol. Oceanogr. Meth.*, 6, 230–235, <https://doi.org/10.4319/lom.2008.6.230>, 2008.
- 785 Druffel, E. R. M., Williams, P. M., Bauer, J. E., and Ertel, J. R.: Cycling of dissolved and particulate organic matter in the open ocean, *Journal of Geophysical Research: Oceans*, 97, 15639–15659, <https://doi.org/10.1029/92JC01511>, 1992.
- Dubois, Michel., Gilles, K. A., Hamilton, J. K., Rebers, P. A., and Smith, Fred.: Colorimetric Method for Determination of Sugars and Related Substances, *Anal. Chem.*, 28, 350–356, <https://doi.org/10.1021/ac60111a017>, 1956.
- Edler, L. and Elbrächter, M.: The Utermöhl method for quantitative phytoplankton analysis, in: *Microscopic and molecular methods for quantitative phytoplankton analysis*, vol. 110, Unesco Pub., 13–20, 2010.
- 790 Eilertsen, H. C., Falk-Petersen, S., Hopkins, C. C. E., and Tande, K.: Ecological investigations on the plankton community of Balsfjorden, northern Norway: program for the project, study area, topography, and physical environment, *Sarsia*, 66, 25–34, 1981.
- Einarsdóttir, K., Attermeyer, K., Hawkes, J. A., Kothawala, D., Sponseller, R. A., and Tranvik, L. J.: Particles and Aeration at Mire-Stream Interfaces Cause Selective Removal and Modification of Dissolved Organic Matter, *Journal of Geophysical Research: Biogeosciences*, 125, e2020JG005654, <https://doi.org/10.1029/2020JG005654>, 2020.
- Engel, A.: The role of transparent exopolymer particles (TEP) in the increase in apparent particle stickiness (α) during the decline of a diatom bloom, *Journal of Plankton Research*, 22, 485–497, 2000.
- Engel, A. and Passow, U.: Carbon and nitrogen content of transparent exopolymer particles (TEP) in relation to their Alcian
800 Blue adsorption, *Marine Ecology Progress Series*, 219, 1–10, <https://doi.org/10.3354/meps219001>, 2001.
- Engel, A., Thoms, S., Riebesell, U., Rochelle-Newall, E., and Zondervan, I.: Polysaccharide aggregation as a potential sink of marine dissolved organic carbon, *Nature*, 428, 929–932, <https://doi.org/10.1038/nature02453>, 2004.
- Flerus, R., Lechtenfeld, O. J., Koch, B. P., McCallister, S. L., Schmitt-Kopplin, P., Benner, R., Kaiser, K., and Kattner, G.:
805 A molecular perspective on the ageing of marine dissolved organic matter, *Biogeosci.*, 9, 1935–1955, <https://doi.org/10.5194/bg-9-1935-2012>, 2012.
- Fonvielle, J. A., Felgate, S. L., Tanentzap, A. J., and Hawkes, J. A.: Assessment of sample freezing as a preservation technique for analysing the molecular composition of dissolved organic matter in aquatic systems, *RSC Advances*, 13, 24594–24603, <https://doi.org/10.1039/D3RA01349A>, 2023.
- Forest, A., Babin, M., Stemmann, L., Picheral, M., Sampei, M., Fortier, L., Gratton, Y., Bélanger, S., Devred, E., Sahlin, J.,
810 Doxaran, D., Joux, F., Ortega-Retuerta, E., Martín, J., Jeffrey, W. H., Gasser, B., and Carlos Miquel, J.: Ecosystem function and particle flux dynamics across the Mackenzie Shelf (Beaufort Sea, Arctic Ocean): an integrative analysis of spatial variability and biophysical forcings, *Biogeosciences*, 10, 2833–2866, <https://doi.org/10.5194/bg-10-2833-2013>, 2013.
- Gruber, D. F., Simjouw, J. P., Seitzinger, S. P., and Taghon, G. L.: Dynamics and characterization of refractory dissolved organic matter produced by a pure bacterial culture in an experimental predator-prey system, *Appl Environ Microbiol*, 72, 4184–491, <https://doi.org/10.1128/aem.02882-05>, 2006.
- 815 Hammer, Ø., Harper, D. A. T., Ryan, P. D.: PAST: Paleontological statistics software package for education and data analysis, , 4, 9 pp, 2001.
- Hansell, D. A.: Recalcitrant Dissolved Organic Carbon Fractions, *Annual Review of Marine Science*, 5, 421–445, <https://doi.org/10.1146/annurev-marine-120710-100757>, 2013a.
- 820 Hansell, D. A.: Recalcitrant dissolved organic carbon fractions, *Ann Rev Mar Sci*, 5, 421–45, <https://doi.org/10.1146/annurev-marine-120710-100757>, 2013b.
- Hansell, D. A., Carlson, C., Repeta, D., and Schlitzer, R.: Dissolved Organic Matter in the Ocean: A Controversy Stimulates New Insights, *Oceanogr.*, 22, 202–211, <https://doi.org/10.5670/oceanogr.2009.109>, 2009.



- 825 He, W., Chen, M., Schlautman, M. A., and Hur, J.: Dynamic exchanges between DOM and POM pools in coastal and inland aquatic ecosystems: A review, *Science of The Total Environment*, 551–552, 415–428, <https://doi.org/10.1016/j.scitotenv.2016.02.031>, 2016.
- Hellebust, J. A.: Excretion of Some Organic Compounds by Marine Phytoplankton, *Limnology and Oceanography*, 10, 192–206, <https://doi.org/10.4319/lo.1965.10.2.0192>, 1965.
- 830 Hertkorn, N., Benner, R., Frommberger, M., Schmitt-Kopplin, P., Witt, M., Kaiser, K., Kettrup, A., and Hedges, J. I.: Characterization of a major refractory component of marine dissolved organic matter, *Geochimica et Cosmochimica Acta*, 70, 2990–3010, <https://doi.org/10.1016/j.gca.2006.03.021>, 2006.
- Hopkinson, C. S. and Vallino, J. J.: Efficient export of carbon to the deep ocean through dissolved organic matter, *Nature*, 433, 142–145, <https://doi.org/10.1038/nature03191>, 2005.
- 835 Iversen, M. H.: Carbon export in the ocean: A biologist’s perspective, *Annu. Rev. Mar. Sci.*, 15, <https://doi.org/10.1146/annurev-marine-032122-035153>, 2023.
- von Jackowski, A., Grosse, J., Nothig, E. M., and Engel, A.: Dynamics of organic matter and bacterial activity in the Fram Strait during summer and autumn, *Philos. Trans. R. Soc. A-Math. Phys. Eng. Sci.*, 378, 16, <https://doi.org/10.1098/rsta.2019.0366>, 2020.
- 840 Jiao, N., Herndl, G. J., Hansell, D. A., Benner, R., Kattner, G., Wilhelm, S. W., Kirchman, D. L., Weinbauer, M. G., Luo, T., Chen, F., and Azam, F.: Microbial production of recalcitrant dissolved organic matter: long-term carbon storage in the global ocean, *Nat Rev Microbiol*, 8, 593–9, <https://doi.org/10.1038/nrmicro2386>, 2010.
- Kepkay, P. E.: Particle aggregation and the biological reactivity of colloids, *Mar. Ecol. Prog. Ser.*, 1994.
- Kerner, M., Hohenberg, H., Ertl, S., Reckermann, M., and Spitzzy, A.: Self-organization of dissolved organic matter to micelle-like microparticles in river water, *Nature*, 422, 150–154, <https://doi.org/10.1038/nature01469>, 2003.
- 845 Kiørboe, T.: Formation and fate of marine snow: small-scale processes with large-scale implications, *Scientia Marina*, 65, 57–71, <https://doi.org/10.3989/scimar.2001.65s257>, 2001.
- Koch, B. P. and Dittmar, T.: From mass to structure: an aromaticity index for high-resolution mass data of natural organic matter, *Rapid Communications in Mass Spectrometry*, 20, 926–932, <https://doi.org/10.1002/rcm.2386>, 2006a.
- 850 Koch, B. P. and Dittmar, T.: From mass to structure: an aromaticity index for high-resolution mass data of natural organic matter, *Rapid Commun. Mass Spectrom.*, 20, 926–932, <https://doi.org/10.1002/rcm.2386>, 2006b.
- Koch, B. P., Witt, M., Engbrodt, R., Dittmar, T., and Kattner, G.: Molecular formulae of marine and terrigenous dissolved organic matter detected by electrospray ionization Fourier transform ion cyclotron resonance mass spectrometry, *Geochimica et Cosmochimica Acta*, 69, 3299–3308, <https://doi.org/10.1016/j.gca.2005.02.027>, 2005.
- 855 Li, X., Skillman, L., Li, D., and Ela, W. P.: Comparison of Alcian blue and total carbohydrate assays for quantitation of transparent exopolymer particles (TEP) in biofouling studies, *Water Research*, 133, 60–68, <https://doi.org/10.1016/j.watres.2017.12.021>, 2018.
- Mague, T. H., Friberg, E., Hughes, D. J., and Morris, I.: Extracellular release of carbon by marine phytoplankton; a physiological approach, *Limnology and Oceanography*, 25, 262–279, <https://doi.org/10.4319/lo.1980.25.2.0262>, 1980.
- 860 Maie, N., Pisani, O., and Jaffé, R.: Mangrove tannins in aquatic ecosystems: Their fate and possible influence on dissolved organic carbon and nitrogen cycling, *Limnology and Oceanography*, 53, 160–171, <https://doi.org/10.4319/lo.2008.53.1.0160>, 2008.
- Mari, X. and Burd, A.: Seasonal size spectra of transparent exopolymeric particles (TEP) in a coastal sea and comparison with those predicted using coagulation theory, *Marine Ecology Progress Series*, 163, 63–76, <https://doi.org/10.3354/meps163063>, 1998.
- 865 Marquardt, M., Vader, A., Stübner, E. I., Reigstad, M., and Gabrielsen, T. M.: Strong Seasonality of Marine Microbial Eukaryotes in a High-Arctic Fjord (Isfjorden, in West Spitsbergen, Norway), *Applied and Environmental Microbiology*, 82, 1868–1880, <https://doi.org/10.1128/AEM.03208-15>, 2016.
- Medeiros, P. M., Seidel, M., Niggemann, J., Spencer, R. G. M., Hernes, P. J., Yager, P. L., Miller, W. L., Dittmar, T., and Hansell, D. A.: A novel molecular approach for tracing terrigenous dissolved organic matter into the deep ocean, *Global Biogeochemical Cycles*, 30, 689–699, <https://doi.org/10.1002/2015GB005320>, 2016.
- 870 Moran, M. A., Kujawinski, E. B., Schroer, W. F., Amin, S. A., Bates, N. R., Bertrand, E. M., Braakman, R., Brown, C. T., Covert, M. W., Doney, S. C., Dyrhman, S. T., Edison, A. S., Eren, A. M., Levine, N. M., Li, L., Ross, A. C., Saito, M. A.,



- 875 Santoro, A. E., Segrè, D., Shade, A., Sullivan, M. B., and Vardi, A.: Microbial metabolites in the marine carbon cycle, *Nature Microbiology*, 7, 508–523, <https://doi.org/10.1038/s41564-022-01090-3>, 2022.
- Myklestad, S. M.: Release of extracellular products by phytoplankton with special emphasis on polysaccharides, *Science of The Total Environment*, 165, 155–164, [https://doi.org/10.1016/0048-9697\(95\)04549-G](https://doi.org/10.1016/0048-9697(95)04549-G), 1995.
- 880 Nguyen, H. T., Lee, Y. M., Hong, J. K., Hong, S., Chen, M., and Hur, J.: Climate warming-driven changes in the flux of dissolved organic matter and its effects on bacterial communities in the Arctic Ocean: A review, *Frontiers in Marine Science*, 9, <https://doi.org/10.3389/fmars.2022.968583>, 2022.
- Orellana, M. V. and Leck, C.: Marine Microgels, in: *Biogeochemistry of Marine Dissolved Organic Matter*, Elsevier, 451–480, <https://doi.org/10.1016/B978-0-12-405940-5.00009-1>, 2015.
- O’Sadnick, M., Petrich, C., Brekke, C., and Skarðhamar, J.: Ice extent in sub-arctic fjords and coastal areas from 2001 to 2019 analyzed from MODIS imagery, *Annals of Glaciology*, 1–17, <https://doi.org/10.1017/aog.2020.34>, 2020.
- 885 Osterholz, H., Dittmar, T., and Niggemann, J.: Molecular evidence for rapid dissolved organic matter turnover in Arctic fjords, *Marine Chemistry*, 160, 1–10, <https://doi.org/10.1016/j.marchem.2014.01.002>, 2014.
- Parsons, T. R., Maita, Y., and Lalli, C. M.: Fluorometric Determination of Chlorophylls, in: *A Manual of Chemical & Biological Methods for Seawater Analysis*, edited by: Parsons, T. R., Maita, Y., and Lalli, C. M., Pergamon, Amsterdam, 107–109, <https://doi.org/10.1016/B978-0-08-030287-4.50034-7>, 1984.
- 890 Passow, U.: Formation of transparent exopolymer particles, TEP, from dissolved precursor material, *Marine Ecology Progress Series*, 192, 1–11, <https://doi.org/10.3354/meps192001>, 2000.
- Passow, U.: Production of transparent exopolymer particles (TEP) by phyto- and bacterioplankton, *Mar. Ecol. Prog. Ser.*, 236, 1–12, <https://doi.org/10.3354/meps236001>, 2002a.
- Passow, U.: Transparent exopolymer particles (TEP) in aquatic environments, *Prog. Oceanogr.*, 55, 287–333, [https://doi.org/10.1016/S0079-6611\(02\)00138-6](https://doi.org/10.1016/S0079-6611(02)00138-6), 2002b.
- 895 Passow, U. and Alldredge, A. L.: A dye-binding assay for the spectrophotometric measurement of transparent exopolymer particles (TEP), *Limnology and Oceanography*, 40, 1326–1335, <https://doi.org/10.4319/lo.1995.40.7.1326>, 1995.
- Passow, U., Alldredge, A. L., and Logan, B. E.: The role of particulate carbohydrate exudates in the flocculation of diatom blooms, *Deep Sea Research Part I: Oceanographic Research Papers*, 41, 335–357, [https://doi.org/10.1016/0967-0637\(94\)90007-8](https://doi.org/10.1016/0967-0637(94)90007-8), 1994.
- 900 Paulsen, M. L., Seuthe, L., Reigstad, M., Larsen, A., Cape, M., and Vernet, M.: Asynchronous Accumulation of Organic Carbon and Nitrogen in the Atlantic Gateway to the Arctic Ocean, 2296–7745, <https://doi.org/10.3389/fmars.2018.00416>, 2018.
- Paulsen, M. L., Müller, O., Larsen, A., Møller, E. F., Middelboe, M., Sejr, M. K., and Stedmon, C.: Biological transformation of Arctic dissolved organic matter in a NE Greenland fjord, *Limnology and Oceanography*, 64, 1014–1033, <https://doi.org/10.1002/lno.11091>, 2019.
- 905 Petersen, G. H. and Curtis, M. A.: Differences in energy flow through major components of subarctic, temperate and tropical marine shelf ecosystems, *Dana*, 1, 53–64, 1980.
- Pisani, O., Yamashita, Y., and Jaffé, R.: Photo-dissolution of flocculent, detrital material in aquatic environments: Contributions to the dissolved organic matter pool, *Water Research*, 45, 3836–3844, <https://doi.org/10.1016/j.watres.2011.04.035>, 2011.
- 910 R Core Team: R: A Language and Environment for Statistical Computing, R Foundation for Statistical Computing, Vienna, Austria, 2018.
- Repeta, D. J.: Chemical Characterization and Cycling of Dissolved Organic Matter, in: *Biogeochemistry of Marine Dissolved Organic Matter*, Elsevier, 21–63, <https://doi.org/10.1016/B978-0-12-405940-5.00002-9>, 2015.
- 915 Retelletti Brogi, S., Jung, J. Y., Ha, S.-Y., and Hur, J.: Seasonal differences in dissolved organic matter properties and sources in an Arctic fjord: Implications for future conditions, *Science of The Total Environment*, 694, 133740, <https://doi.org/10.1016/j.scitotenv.2019.133740>, 2019.
- Riebesell, U., Reigstad, M., Wassmann, P., Noji, T., and Passow, U.: On the trophic fate of *Phaeocystis pouchetii* (hariot): VI. Significance of *Phaeocystis*-derived mucus for vertical flux, *Neth. J. Sea Res.*, 33, [https://doi.org/10.1016/0077-7579\(95\)90006-3](https://doi.org/10.1016/0077-7579(95)90006-3), 1995.
- 920 Riley, G. A.: Organic Aggregates in Seawater and the Dynamics of Their Formation and Utilization, *Limnology and Oceanography*, 8, 372–381, <https://doi.org/10.4319/lo.1963.8.4.0372>, 1963.



- 925 Sheldon, R. W., Evelyn, T. P. T., and Parsons, T. R.: On the Occurrence and Formation of Small Particles in Seawater, *Limnology and Oceanography*, 12, 367–375, <https://doi.org/10.4319/lo.1967.12.3.0367>, 1967.
- Sleighter, R. L. and Hatcher, P. G.: Molecular characterization of dissolved organic matter (DOM) along a river to ocean transect of the lower Chesapeake Bay by ultrahigh resolution electrospray ionization Fourier transform ion cyclotron resonance mass spectrometry, *Marine Chemistry*, 110, 140–152, <https://doi.org/10.1016/j.marchem.2008.04.008>, 2008.
- 930 Suttle, C. A.: Marine viruses — major players in the global ecosystem, *Nature Reviews Microbiology*, 5, 801–812, <https://doi.org/10.1038/nrmicro1750>, 2007.
- Svensen, C. and Vernet, M.: Production of dissolved organic carbon by *Oithona nana* (Copepoda: Cyclopoida) grazing on two species of dinoflagellates, *Mar Biol*, 163, 237, <https://doi.org/10.1007/s00227-016-3005-9>, 2016.
- Thornton, D. C. O.: Diatom aggregation in the sea: mechanisms and ecological implications, *Euro. J. Phycol.*, 37, 149–161, <https://doi.org/10.1017/S0967026202003657>, 2002.
- 935 Thornton, D. C. O.: Dissolved organic matter (DOM) release by phytoplankton in the contemporary and future ocean, *European Journal of Phycology*, 49, 20–46, <https://doi.org/10.1080/09670262.2013.875596>, 2014.
- Timko, S. A., Gonsior, M., and Cooper, W. J.: Influence of pH on fluorescent dissolved organic matter photo-degradation, *Water Research*, 85, 266–274, <https://doi.org/10.1016/j.watres.2015.08.047>, 2015.
- 940 Turner, J. T.: Zooplankton fecal pellets, marine snow, phytodetritus and the ocean’s biological pump, *Prog. Oceanogr.*, 130, <https://doi.org/10.1016/j.pocean.2014.08.005>, 2015.
- Utermöhl, H.: Zur Vervollkommnung der quantitativen Phytoplankton-Methodik, *SIL Communications*, 1953-1996, 9, <https://doi.org/10.1080/05384680.1958.11904091>, 1958.
- Valdes Villaverde, P., Almeda Jauregui, C., and Maske, H.: Rapid abiotic transformation of marine dissolved organic material to particulate organic material in surface and deep waters, *Biogeochemistry: Organic Biogeochemistry*, 945 <https://doi.org/10.5194/bg-2020-291>, 2020.
- Verdugo, P., Alldredge, A. L., Azam, F., Kirchman, D. L., Passow, U., and Santschi, P. H.: The oceanic gel phase: a bridge in the DOM–POM continuum, *Marine Chemistry*, 92, 67–85, <https://doi.org/10.1016/j.marchem.2004.06.017>, 2004.
- Vernet, M., Matrai, P. A., and Andreassen, I.: Synthesis of particulate and extracellular carbon by phytoplankton at the marginal ice zone in the Barents Sea, *Journal of Geophysical Research: Oceans*, 103, 1023–1037, 950 <https://doi.org/10.1029/97JC02288>, 1998.
- Vonnahme, T. R., Klausen, L., Bank, R. M., Michellod, D., Lavik, G., Dietrich, U., and Gradinger, R.: Light and freshwater discharge drive the biogeochemistry and microbial ecology in a sub-Arctic fjord over the Polar night, *Front. Mar. Sci.*, 9, 915192, <https://doi.org/10.3389/fmars.2022.915192>, 2022.
- 955 Wagner, S., Schubotz, F., Kaiser, K., Hallmann, C., Waska, H., Rossel, P. E., Hansman, R., Elvert, M., Middelburg, J. J., Engel, A., Blattmann, T. M., Catalá, T. S., Lennartz, S. T., Gomez-Saez, G. V., Pantoja-Gutiérrez, S., Bao, R., and Galy, V.: Soothsaying DOM: A Current Perspective on the Future of Oceanic Dissolved Organic Carbon, *Front. Mar. Sci.*, 7, <https://doi.org/10.3389/fmars.2020.00341>, 2020.
- Walker, E. Z., Wiedmann, I., Nikolopoulos, A., Skarðhamar, J., Jones, E. M., and Renner, A. H. H.: Pelagic ecosystem dynamics between late autumn and the post spring bloom in a sub-Arctic fjord, *Elementa: Science of the Anthropocene*, 960 10, 00070, <https://doi.org/10.1525/elementa.2021.00070>, 2022.
- Wells, M. L.: Marine colloids: A neglected dimension, *Nature*, 391, 530–531, <https://doi.org/10.1038/35248>, 1998.
- Wetz, M. S. and Wheeler, P. A.: Release of dissolved organic matter by coastal diatoms, *Limnology and Oceanography*, 52, 798–807, <https://doi.org/10.4319/lo.2007.52.2.0798>, 2007.
- 965 Wietz, M., Bienhold, C., Metfies, K., Torres-Valdés, S., von Appen, W.-J., Salter, I., and Boetius, A.: The polar night shift: seasonal dynamics and drivers of Arctic Ocean microbiomes revealed by autonomous sampling, *ISME COMMUN.*, 1, 1–12, <https://doi.org/10.1038/s43705-021-00074-4>, 2021.
- Xu, H. and Guo, L.: Intriguing changes in molecular size and composition of dissolved organic matter induced by microbial degradation and self-assembly, *Water Research*, 135, 187–194, <https://doi.org/10.1016/j.watres.2018.02.016>, 2018.